Electrophilic Activation of Aliphatic C−H Bonds Mediated by Zirconium Hydride Entities and Applied to the Functionalization of the Porphyrinogen Periphery

Denis Jacoby,[†] Sylviane Isoz,[†] Carlo Floriani,*[,†] Angiola Chiesi-Villa,[‡] and Corrado Rizzoli[‡]

Contribution from the Institut de Chimie Minérale et Analytique, BCH, Université de Lausanne, CH-1015 Lausanne, Switzerland, and Dipartimento di Chimica, Università di Parma, I-43100 Parma, Italy

Received October 31, 1994[⊗]

Abstract: A novel mode of electrophilic activation of aliphatic C−H bonds, assisted by zirconium(IV) and achieved by the use of an excess of MH [M = Li, Na, K], allows the functionalization of the periphery of *meso*-octaethylporphyrinogen. The reaction of $[(\eta^5\text{-}\eta^1\text{-}\eta^5\text{-}\eta^1\text{-}Et_8N_4)Zr(THF)]$ (**1**) with LiH (excess) and NaH (excess) led to the formation of $[\{\eta^1\text{-}\eta^1\text{-}\eta^1\text{-}\eta^5\text{-}Et_7(CH_2CH_2)N_4\}ZrH\{Li(THF)\}_2]$ (**2**) and $[\{\eta^1\text{-}\eta^1\text{-}\eta^1\text{-}\eta^5\text{-}Et_7(CH_2CH_2)N_4\}ZrH\{Na(THF)_2\}_2]$ (**3**), containing a Zr−C bond, derived from the metalation of one of the *meso* ethyl groups, and a triply bridged hydrido ligand. The analogous potassium derivative, $[\{\eta^1\text{-}\eta^1\text{-}\eta^1\text{-}\eta^5\text{-}Et_7(CH_2CH_2)N_4\}ZrH\{K(THF)_2\}_2]$ (**4**), has been obtained only from a metathesis reaction reacting **2** with KH at room temperature. The reaction of **1** with an excess of KH under drastic conditions gave a mixture of dimetalated forms derived from the metalation of two ethyl groups, they are $[\{\eta^1\text{-}\eta^1\text{-}\eta^1\text{-}\eta^1\text{-}Et_6(\overline{CHCH_3})_2N_4\}Zr\{K(THF)_2\}_2]$ (**5**) (75%) and $[\{\eta^1\text{-}\eta^1\text{-}\eta^1\text{-}\eta^1\text{-}Et_6(\overline{CH_2CH_2})_2N_4\}Zr\{K(THF)_2\}_2]$ (**6**) (25%). The conversion of **4** into a mixture of **5** and **6** has been observed in the presence of an excess of KH under forcing conditions. Such a conversion gives some insight into the metalation mechanism. In particular, the transformation of **4** into **5** and **6** suggests a facile Zr−C and C−H σ-bond metathesis. The insertion of Bu^tNC into the Zr−C bond of **2** led to the formation of an η^2-iminoacyl, $[\{\eta^1\text{-}\eta^1\text{-}\eta^1\text{-}\eta^5\text{-}Et_7(CH_2CH_2\text{-}\eta^2\text{-}C{=}NBu^t)\}ZrH\{Li(THF)\}_2]$ (**7**), which undergoes, in water, a hydrolytic cyclization to $[Et_7(\overline{CH_2CH_2COC_4H_4N})(C_4H_2NH)_3]$ (**9**) via the attack of a carbenium η^2-iminoacyl on one of the pyrrolyl anions. The intermediacy of such a migrated carbenium η^2-iminoacyl has been observed during the controlled protolysis of **7** in aprotic solvents using $PhNH_2{\cdot}HCl$, which led to the isolation of $[\eta^1\text{-}\eta^1\text{-}\eta^5\text{-}\eta^1\text{-}Et_7(\overline{CH_2CH_2C(NBu^t)C_4H_4N})(C_4H_2N)_3ZrNHPh]$ (**10**). The spontaneous migration of a carbenium η^2-acyl from the metal to a pyrrolyl anion has been observed in the reaction of **2** with either carbon monoxide or $[Mo(CO)_6]$. Both reactions led, via intermediates very similar to **9** and **10**, to the homologation of a pyrrole ring and the cleavage of the C−O bond. The resulting zirconyl compound $[\eta^1\text{-}\eta^1\text{-}\eta^5\text{-}\eta^1\text{-}Et_7(C_4H_2N)_3(\overline{CH_2CH_2C_5H_2N})Zr{=}O{-}Li]_2$ (**11**) has been isolated as a dimer. The reaction of **2** with Bu^tNC and CO emphasizes how the direct functionalization of an aliphatic chain in porphyrinogen chemistry can be achieved and used for synthetic purposes. Crystallographic details: The compound **2** is triclinic, space group $P\bar{1}$, a = 11.394(4) Å, b = 20.135(5) Å, c = 10.791(3) Å, α = 103.34(2)°, β = 117.88(2)°, γ = 79.27(2)°, Z = 2, and R = 0.048. The mixture of **5** + **6** is monoclinic, space group $C2/c$, a = 14.090(1) Å, b = 17.366(2) Å, c = 21.365(3) Å, $\alpha = \gamma$ = 90°, β = 91.84(1)°, Z = 4, and R = 0.045. The compound **7** is monoclinic, space group $P2_1/n$, a = 12.152(2) Å, b = 20.190(3) Å, c = 20.039(3) Å, $\alpha = \gamma$ = 90°, β = 103.39(2)°, Z = 4, and R = 0.041. Compound **10** is monoclinic, space group $P2_1/c$, a = 10.325(2) Å, b = 19.824(3) Å, c = 21.114(4) Å, $\alpha = \gamma$ = 90°, β = 102.72(2)°, Z = 4, and R = 0.060. Compound **11** is monoclinic, space group $P2_1/n$, a = 14.774(4) Å, b = 17.745(5) Å, c = 15.771(4) Å, $\alpha = \gamma$ = 90°, β = 101.55(2)°, Z = 2, and R = 0.067.

Introduction

Although electrophilic metal-mediated aliphatic C−H cleavage is precedented in the literature,[1] its application to the functionalization of complex substrates is almost unknown. The present report deals with a novel electrophilic C−H bond activation and its application to the functionalization of the porphyrinogen skeleton.

Unlike the usual approach, in which a metal-bonded alkyl or hydride is employed to remove an aliphatic hydrogen in intra- or intermolecular processes,[2] we explored the following strategy (eq 1). The removal of an aliphatic hydrogen by an alkali

$$L_nM + RH + M^*H \xrightarrow{-H_2} L_nM(R\cdots M^*) \qquad (1)$$

hydride M*H assisted by an electrophilic metal leads to the formation of a polar alkali metal···alkyl species complexed by L_nM.

Reaction 1 occurs when specific demands are satisfied by the ligand environment of M, particularly that allowing the L_nM complex to behave in a bifunctional manner.[3] This allows for the complexation of alkali hydrides by the concerted action of

[†] Université de Lausanne.
[‡] Università di Parma.
[⊗] Abstract published in *Advance ACS Abstracts*, February 15, 1995.

(1) (a) Davies, J. A.; Watson, P. L.; Liebman, J. F. Greenberg, A. *Selective Hydrocarbon Activation*; VCH: New York, 1990. (b) *Activation and Functionalization of Alkanes*; Hill, C. L., Ed.; Wiley: New York, 1989. (c) Shilov, A. E. *Activation of Saturated Hydrocarbons by Transition Metal Complexes*; Reidel: Hingham, MA, 1984. (d) Jones, W. D.; Feher, F. J. *Acc. Chem. Res.* **1989**, *2*, 91. (e) Ryabov, A. D. *Chem. Rev.* **1990**, *90*, 403. (f) Sen, A. *Acc. Chem. Res.* **1988**, *21*, 421. (g) Crabtree, R. H. *Chem. Rev.* **1985**, *85*, 245.

(2) (a) Rothwell, I. P. *The Homogeneous Activation of Carbon-Hydrogen Bonds by Electrophilic Metal Systems*; Chapter 3 in ref 1a. (b) Watson, P. L. *C-H Bond Activation with Complexes of Lanthanides and Actinide Elements*; Chapter 4 in ref 1a. (c) Rothwell, I. P. *The Homogeneous Activation of Carbon-Hydrogen Bonds by High Valent Early d-Block, Lanthanides and Actinide Metal Systems*; Chapter 5 in ref 1b.

0002-7863/95/1517-2805$09.00/0

the electron-rich periphery and the electron-deficient metal to be achieved, as well as the complexation of the polar alkyl formed from the reaction.[4] *meso*-Octaethylporphyrinogen provides the appropriate ligand environment to metals for the formation of just such bifunctional complexes.[5] In addition, the calix[*n*]arene-type conformations of the porphyrinogen[6] allow the *meso*-ethyl substituent to approach the metal, so as to assist the intramolecular deprotonation of an alkyl chain. Therefore the process depicted in reaction 1 is achieved intramolecularly. The model complex we have considered for this purpose is the *meso*-octaethylporphyrinogen–zirconium-(IV) complex $[(\eta^5\text{-}\eta^1\text{-}\eta^5\text{-}\eta^1\text{-}Et_8N_4)Zr(THF)]$ (**1**).[4a]

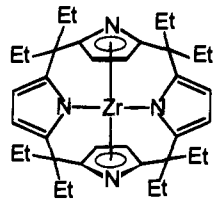

$[(\eta^5\text{-}\eta^1\text{-}\eta^5\text{-}\eta^1\text{-}Et_8N_4)Zr(THF)]$, **1**

The reaction of **1** with stoichiometric amounts of alkali···alkyls and alkali hydrides led to the recently reported bifunctional alkali–zirconium–alkyl $[(\eta^5\text{-}\eta^1\text{-}\eta^1\text{-}\eta^1\text{-}Et_8N_4)ZrR\{M(THF)_n\}]$ (M = Li, Na, K) and hydrido complexes $[\{(\eta^5\text{-}\eta^1\text{-}\eta^5\text{-}\eta^1\text{-}Et_8N_4)\text{-}Zr\}_2(\mu\text{-}MH)_2]$ [M = Na, K].[4] When a large excess of alkali hydride is used, however, the reaction (depending on the alkali cation and the reaction conditions) led to the intramolecular mono- and di-metalation of the *meso*-ethyl chains and to the formation of Zr–C and Zr–H bonds, which can serve to functionalize the porphyrinogen periphery. The introduction of functional groups into the porphyrinogen periphery has been achieved by reacting such Zr–C and Zr–H bonds with isocyanides and carbon monoxide; thus novel kinds of macrocycles have been obtained.

Results and Discussion

Metalation Reactions. We have previously explored the carrier properties of complex **1** toward alkali hydrides and polar organometallics.[4] Such an ability depends on the intrinsic bifunctional nature of porphyrinogen–transition metal complexes, whereby they contain an electrophilic metal in the core of the structure and maintain an electron-rich periphery available for binding cations, such as alkali cations.[4-7] This bifunctionality of the porphyrinogen–metal complexes is exemplified by the complexation of NaH, KH, and LiR by **1**. In several such complexes, the X-ray structural determination revealed a very interesting close approach of the *meso*-ethyl groups to either the transition metal or the alkali cation. The reaction of **1** with stoichiometric amounts of NaH or KH led to dimeric complexes in which two molecules of **1** sandwich two MH units, with the hydride interacting with zirconium and the alkali cation remaining bonded to the pyrrolyl anions.[4]

When **1** is reacted with a large excess of metal hydride for 2–3 days at 70–100 °C (see Experimental Section), the resultant products are shown in reaction 2.

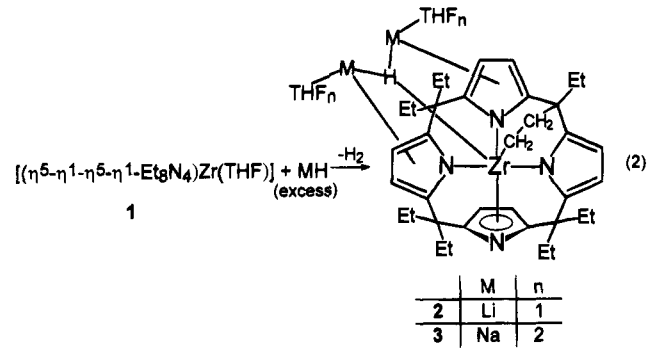

This reaction should be carried out strictly under the conditions reported in the Experimental Section, with particular emphasis on certain factors, such as the large excess of MH, the solvents, the reaction time, and the use of a gentle vacuum serving to remove H_2 from the reaction. Compounds **2** and **3** exhibit the same structures, as determined by the X-ray analyses.

Two possible routes for the formation of **2** and **3** have been considered. One involves the intermediate formation of a dihydrido species, followed by the intramolecular loss of H_2 from the hydride and one of the ethyl groups.

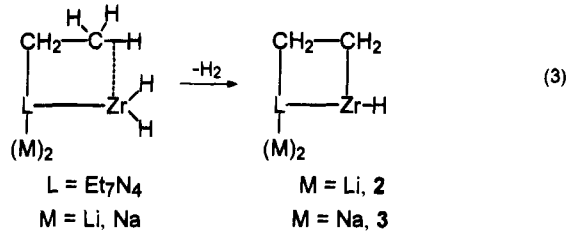

An alternative pathway is the intermolecular deprotonation of the aliphatic chain activated by the acidic zirconium(IV).[8] In such complexes it is known that the ethyl groups are conformationally forced to approach the metal.[4,5,7]

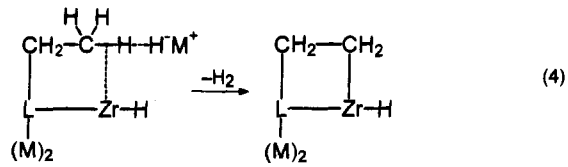

The binding of the alkali cation by the porphyrinogen periphery would then favor the deprotonation by an external hydride source. However, it is difficult to distinguish between these two possible pathways, though our current preference for the second one is mainly based on steric considerations and on the necessity to use a large excess of MH. When reaction 2 was performed using KH, the mixture of **4** and **5** + **6** (*vide infra*) was obtained. Therefore we found that the best way to synthesize **4**, $[\{\eta^1\text{-}\eta^1\text{-}\eta^5\text{-}Et_7(CH_2\text{-}CH_2)N_4\}Zr\text{-}H\text{-}\{K(THF)_2\}_2]$,

(3) Quan, R. W.; Bazan, G. C.; Kiely, A. F.; Schaefer, W. P.; Bercaw, J. E. *J. Am. Chem. Soc.* **1994**, *116*, 4489.

(4) (a) Jacoby, D.; Floriani, C.; Chiesi-Villa, A.; Rizzoli, C. *J. Am. Chem. Soc.* **1993**, *115*, 3595. (b) Jacoby, D.; Floriani, C.; Chiesi-Villa, A.; Rizzoli, C. *J. Am. Chem. Soc.* **1993**, *115*, 7025.

(5) (a) Jacoby, D.; Floriani, C.; Chiesi-Villa, A.; Rizzoli, C. *J. Chem. Soc., Chem. Commun.* **1991**, 220. (b) Jubb, J.; Jacoby, D.; Floriani, C.; Chiesi-Villa, A.; Rizzoli, C. *Inorg. Chem.* **1992**, *31*, 1306.

(6) (a) von Maltzan, B. *Angew. Chem., Int. Ed. Engl.* **1982**, *21*, 785. (b) Gutsche, C. D. *Calixarenes*; Royal Society of Chemistry: Cambridge, U.K., 1989.

(7) (a) Jacoby, D.; Floriani, C.; Chiesi-Villa, A.; Rizzoli, C. *J. Chem. Soc., Chem. Commun.* **1991**, 790. (b) Jubb, J.; Floriani, C.; Chiesi-Villa, A.; Rizzoli, C. *J. Am. Chem. Soc.* **1992**, *114*, 6571. (c) De Angelis, S.; Solari, E.; Floriani, C.; Chiesi-Villa, A.; Rizzoli, C. *J. Chem. Soc., Dalton Trans.* **1994**, 2467. (d) Piarulli, U.; Floriani, C.; Chiesi-Villa, A.; Rizzoli, C. *J. Chem. Soc., Chem. Commun.*, **1994**, 895. (e) De Angelis, S.; Solari, E.; Floriani, C.; Chiesi-Villa, A.; Rizzoli, C. *J. Am. Chem. Soc.* **1994**, *116*, 5691 and 5702. (f) Solari, E.; Musso, F.; Floriani, C.; Chiesi-Villa, A.; Rizzoli, C. *J. Chem. Soc., Dalton Trans.* **1994**, 2015.

(8) How, in some rigid conformations of the porphyrinogen-type skeleton we can get C–H bonds acting as ligands for an electrophilic metal has been recently disclosed: Kretz, C. M.; Gallo, E.; Solari, E.; Floriani, C.; Chiesi-Villa, A.; Rizzoli, C. *J. Am. Chem. Soc.* **1994**, *116*, 10775.

was via an alkali cation exchange reaction; thus **4**,[9] having the same structure as **3**, has been obtained by reacting **2** with KH (reaction 5).

$$[\{\eta^1\text{-}\eta^1\text{-}\eta^1\text{-}\eta^5\text{-}Et_7(CH_2\text{-}CH_2)N_4\}Zr\text{-}H\text{-}\{Li(THF)\}_2] \quad \mathbf{2} \xrightarrow{KH} [\{\eta^1\text{-}\eta^1\text{-}\eta^1\text{-}\eta^5\text{-}Et_7(CH_2\text{-}CH_2)N_4\}Zr\text{-}H\text{-}\{K(THF)_2\}_2] \quad \mathbf{4} \qquad (5)$$

The spectroscopic data (IR and NMR) are not particularly informative about the structures of **2**−**4**, except that the NMR spectra provide an initial fingerprint of the structure. Because the crystal structures of **2**−**4** are very similar, the following discussion will be confined to the structure of **2** only. Figures 1A and 1B show partial and complete views, respectively, of complex **2**. Figure 1A contains the numbering scheme which will be used for the porphyrinogen skeleton from now on. Within the text the pyrrole rings containing N1, N2, N3, and N4 will be referred to as rings A, B, C, and D, respectively. Selected interatomic distances are listed in Table 2. A comparison of the most relevant conformational parameters for the present series of compounds is given in Table 7. The porphyrinogen exhibits a η^5-η^1-η^1-η^1 bonding mode and a β-metalation of the C27−C28 ethyl chain. The β-metalation gives rise to two six-membered chelation rings which are folded along the Zr−C10 line, the Zr,C28,C27,C10 least-squares mean plane forming dihedral angles of 68.9(2)° and 60.4(2)° with the Zr,N2,C9,C10 and Zr,N3,C11,C10 least-squares mean planes. The Zr,C28,C27,C10 mean plane is almost perpendicular to the N_4 core, the dihedral angle they form being 83.2(2)°. The N_4 core shows significant tetrahedral distortions (Table 7) with the Zr atom protruding by 0.593(1) Å. The trend of LiC and LiN distances suggests an η^2-pyrrolyl−Li1 interaction and an η^5-pyrrolyl−Li2 interaction involving the A and B rings, respectively. In addition, the Li1 cation is η^1-bonded to N4 and the Li2 cation shows a weaker interaction with N3. Each lithium cation completes its coordination through the oxygen atom from a THF molecule and the bridging hydride.[4]

Some significant insights into the metalation of the ethyl substituent come from the careful examination of the reaction between **1** and KH under various conditions. The zirconocene hydrido functionality has been around for a long time in organometallic chemistry, and it has been involved in a number of key reactions such as hydrozirconation[10] and the reduction of carbon monoxide.[11] The bonding mode of the hydride to Zr is usually either terminal or bridging. However, an alternative heterodimetallic bridging mode has been observed in the dimeric $[\{(\eta^5\text{-}\eta^1\text{-}\eta^5\text{-}\eta^1\text{-}Et_8N_4)Zr\}_2(\mu\text{-}MH)_2]$ [M = Na, K][4] in complexes **2**, **3**, and **4** and for some other very electrophilic metals, such as Y and Al.[12] This heterodimetallic interaction may be the key factor determining both the strength and the polarization of the metal−hydrogen bond appropriate for the metalation of C−H functionalities. In fact, when the reaction of **1** with KH was carried out under more drastic conditions (1 week at 60 °C) in THF, a mixture of **5** (25%) and **6** (75%) was obtained.

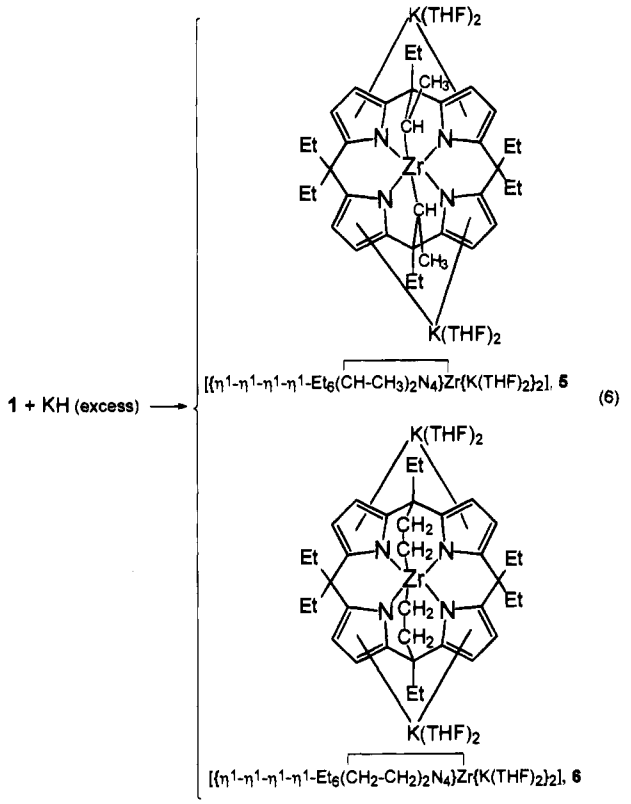

The mixture of **5** and **6** consistently forms regardless of the reaction conditions and of the kind of reaction (*vide infra*). The composition of the isomeric mixture remains constant both in the solid state and in solution, including in the mother liquor when the solid has been filtered out (^{1}H NMR). Because the spectroscopic data were insufficient to elucidate the structures of **5** and **6**, an X-ray structural analysis was performed on a crystal containing the mixture of both compounds. The structures of **5** and **6** are displayed in Figures 2 and 3, respectively, with selected bond parameters reported in Table 3.

Both molecules possess a crystallographically imposed C_2 symmetry, the 2-fold axis running through the zirconium atom perpendicularly to the N_4 core. The disorder affecting the ethyl chains bonded to C5 was interpreted as due to the simultaneous presence of the α- (75%, Figure 2) and β-dimetalated (25%, Figure 3) isomers. Porphyrinogen exhibits a η^1-η^1-η^1-η^1

(9) Crystallographic details for complex **4**: orthorhombic, space group $P2_12_12_1$, a = 19.518(4) Å, b = 21.486(5) Å, c = 12.581(6) Å, $\alpha = \beta = \gamma$ = 90°, Z = 4, and R = 0.048.

(10) Schwartz, J.; Labinger, J. A. *Angew. Chem., Int. Ed. Engl.* **1976**, *15*, 333. Carr, D. B.; Yoshifuji, M.; Shoer, L. I.; Gell, K. I.; Schwartz, J. *Ann. N.Y. Acad. Sci.* **1977**, *295*, 127. Hart, D. W.; Blackburn, T. F.; Schwartz, J. *J. Am. Chem. Soc.* **1975**, *97*, 679. Hart, D. W.; Schwartz, J. *J. Am. Chem. Soc.* **1974**, *96*, 8115. Gibson, T. *Tetrahedron Lett.* **1982**, *23*, 157. Bock, P. L.; Boschetto, D. J.; Rasmussen, J. R.; Demers, J. P.; Whitesides, G. M. *J. Am. Chem. Soc.* **1974**, *96*, 2814. Labinger, J. A.; Hart, D. W.; Seibert, W. E.; Schwartz, J. *J. Am. Chem. Soc.* **1975**, *97*, 3851. Bertelo, C. A.; Schwartz, J. *J. Am. Chem. Soc.* **1976**, *98*, 262; **1975**, *97*, 228. Blackburn, T. F.; Labinger, J. A.; Schwartz, J. *Tetrahedron Lett.* **1975**, *16*, 3041. Neghishi, E.; Yoshida, T. *Tetrahedron Lett.* **1980**, *21*, 1501. Neghishi, E.; Takahashi, T. *Aldrichimica Acta* **1985**, *18*, 31. Neghishi, E.; Miller, J. A.; Yoshida, T. *Tetrahedron Lett.* **1984**, *25*, 3407. Jordan, R. F.; Lapointe, R. E.; Bradley, P. K.; Baenzinger, N. *Organometallics* **1989**, *8*, 2892 and references therein. For a survey of group IV and V hydrides, see: Toogood, G. E.; Wallbridge, M. G. H. *Adv. Inorg. Chem. Radiochem.* **1982**, *25*, 267. Cardin, D. J.; Lappert, M. F.; Raston, C. L. In *Comprehensive Organometallic Chemistry*; Wilkinson, G., Stone, F. G. A., Abel, E. W., Eds.; Pergamon: Oxford, 1981; Vol. 3, Chapter 23.2, p 45. Schwartz, J. *Pure Appl. Chem.* **1980**, *52*, 733. Buchwald, S. L.; La Maire, S. J.; Nielsen, R. B.; Watson, B. T.; King, S. M. *Tetrahedron Lett.* **1987**, *28*, 3895.

(11) (a) Durfee, L. D.; Rothwell, I. P. *Chem. Rev.* **1988**, *88*, 1059. (b) Wolczanski, P. T.; Bercaw, J. E. *Acc. Chem. Res.* **1980**, *13*, 121. (c) Headford, C. E. L.; Roper, W. R. In *Reactions of Coordinated Ligands*; Braterman, P. S., Ed., Plenum: New York, 1986; Vol. 1, Chapter 8. (d) Cardin, D. J.; Lappert, M. F.; Raston, C. L. *Chemistry of Organo-Zirconium and -Hafnium Compounds*; Ellis Horwood: Chichester, U.K., 1986. (e) Labinger, J. A. *Transition Metal Hydrides*; Dedieu, A., Ed.; VCH: Weinheim, Germany, 1992.

(12) (a) Evans, M. J.; Meadows, H. J.; Hanusa, P. T. *J. Am. Chem. Soc.* **1984**, *106*, 4454. (b) Wailes, P. C.; Weigold, H.; Bell, A. P. *J. Organometal. Chem.* **1972**, *43*, C29.

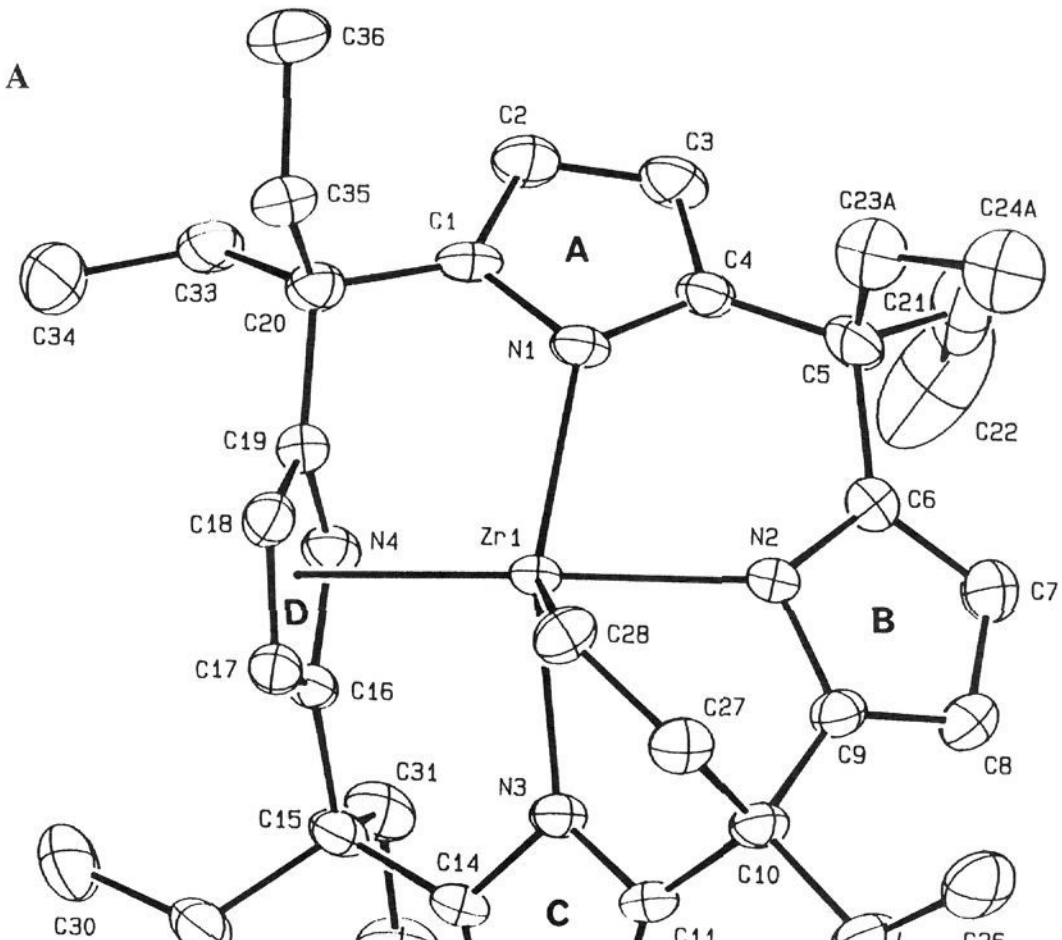

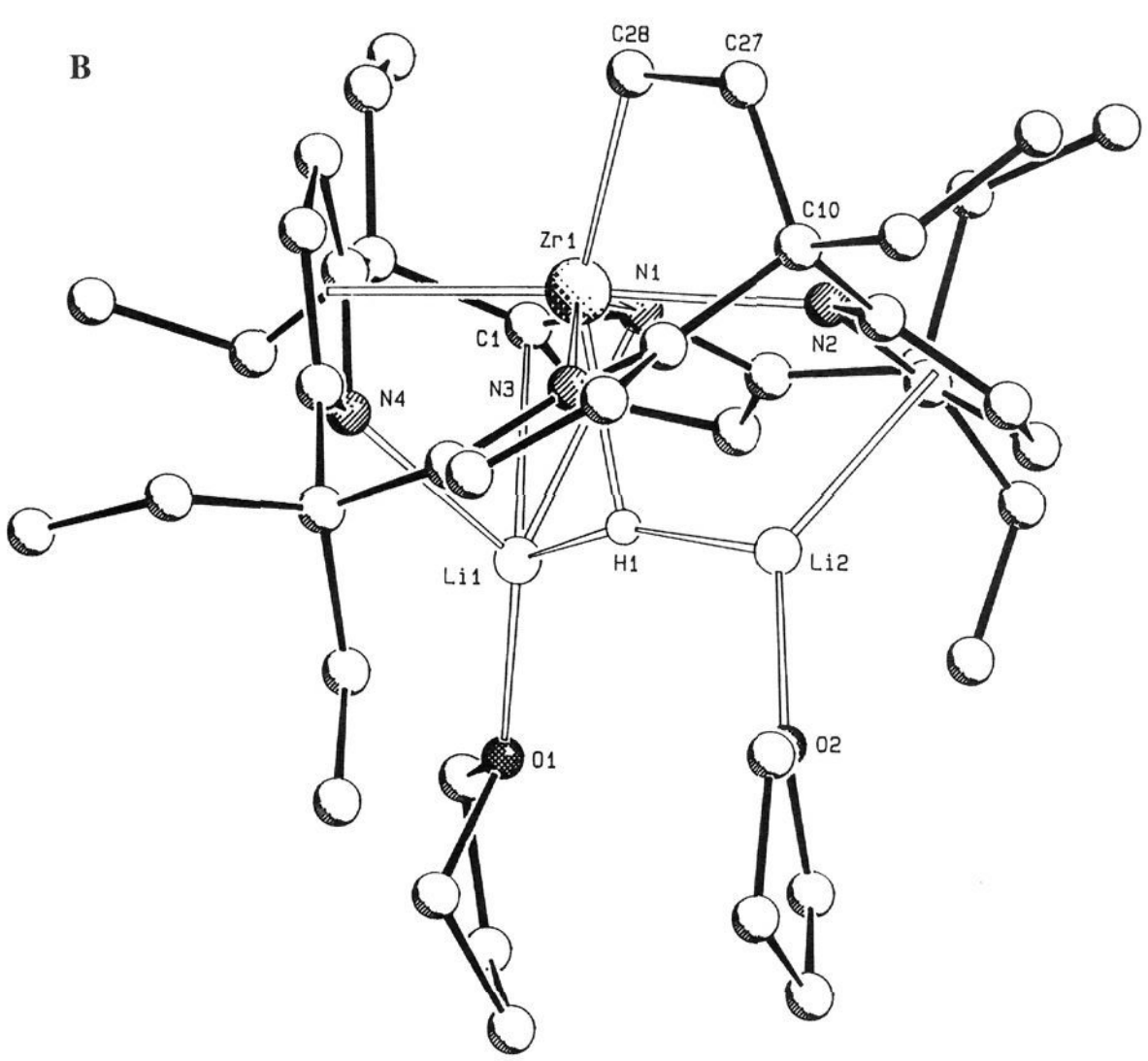

Figure 1. (A) ORTEP drawing of the anion in complex **2** (30% probability ellipsoids). Disorder omitted for clarity. (B) SCHAKAL drawing of complex **2**. Disorder omitted for clarity.

bonding mode. The N_4 core is planar, with the zirconium atom displaced by 0.851(1) Å, a value which is in agreement with that found in the alkylated derivatives.[4a] The Zr−C bond distances have conventional values.[11d] The α-dimetalation gives rise to two five-membered chelate rings which exhibit an envelope conformation, C11A being displaced by 0.995(6) and 1.085(6) Å from the Zr,N1,C4,C5 and Zr,N2,C6,C5 planes, respectively. The β-dimetalation in **6** gives rise to two six-membered chelate rings which are folded along the Zr−C5 line with the Zr,C12B,C11B,C5 least-squares mean plane forming dihedral angles of 59.5(5)° and 55.4(4)° (narrower than those found in **2**) with the Zr,N1,C4,C5 and Zr1,N2,C6,C5 planes. It is also perpendicular to the N_4 core forming a dihedral angle of 91.5(4)°. The Zr,N1,C4,C5,C6,N2 chelate ring assumes a boat

Table 1. Experimental Data for the X-ray Diffraction Studies on Crystalline Compounds **2**, **5** + **6**, **7**, **10**, and **11**[a]

	2	**5 + 6**	**7**	**10**	**11**
formula	$C_{44}H_{64}Li_2N_4O_2Zr$	$C_{52}H_{78}K_2N_4O_4Zr$	$C_{49}H_{73}Li_2N_5O_2Zr$	$C_{47}H_{64}N_6Zr$	$C_{74}H_{94}Li_2N_8O_2Zr_2{\cdot}1.2(C_7H_8)$
a, Å	11.394(4)	14.090(1)	12.152(2)	10.325(2)	14.774(4)
b, Å	20.135(5)	17.366(2)	20.190(3)	19.824(3)	17.745(5)
c, Å	10.791(3)	21.365(3)	20.039(3)	21.114(4)	15.771(4)
α, (deg)	103.34(2)	90	90	90	90
β, (deg)	117.88(2)	91.84(1)	103.39(2)	102.72(2)	101.55(2)
γ, (deg)	79.27(2)	90	90	90	90
V, Å^3	2120.4(12)	5225.0(10)	4782.9(13)	4215.6(14)	4050.9(19)
Z	2	4	4	4	2
fw	786.1	992.6	869.3	804.3	1434.5
space group	$P\bar{1}$ (No. 2)	*C*2/*c* (No. 15)	$P2_1/n$ (No. 14)	$P2_1/c$ (No. 14)	$P2_1/n$ (No. 14)
t, °C	22	22	22	22	22
λ, Å	0.71069	0.71069	1.54178	0.71069	0.71069
ϱ_{calc}, g cm^{-3}	1.231	1.262	1.207	1.267	1.176
μ, cm^{-1}	2.9	4.1	22.00	2.93	2.98
transmn coeff	0.965−1.000	0.947−1.000	0.780−1.000	0.954−1.000	0.904−1.000
R[b]	0.048	0.045	0.041	0.060	0.067
wR2[c]	0.140	0.127	0.110	0.138	0.162
GOF	0.969	1.057	0.823	1.043	1.087

[a] $R = \sum|\Delta F|/\sum|F_o|$. $wR2 = [\sum(w\Delta F^2)^2/\sum wF_o^2)^2]^{1/2}$. $GOF = [\sum w|\Delta F|^2/(NO - NV)]^{1/2}$. [b] For the unique observed data for all compounds. [c] For the unique total data for **2**, **5**+**6**, **7**; for the unique observed data for **10** and **11**.

Table 2. Selected Interatomic Distances (Å) and Angles (deg) for Complex **2**[a]

Zr1−N1	2.253(3)	Zr1−C16	2.510(5)
Zr1−N2	2.229(4)	Zr1−C17	2.618(4)
Zr1−N3	2.222(4)	Zr1−C18	2.624(4)
Zr1−N4	2.432(4)	Zr1−C19	2.498(4)
Zr1−C28	2.294(5)	Zr1−Cp4	2.245(4)
Li1−O1	1.869(9)	Zr1−H1	2.09
Li2−O2	1.893(14)	Li1−H1	1.85
		Li2−H1	1.82
Li1−N1	2.471(13)	Li2−N2	2.303(14)
Li1−C1	2.468(14)	Li2−C6	2.514(16)
Li1−C2	2.925(14)	Li2−C7	2.600(15)
Li1−C3	3.168(15)	Li2−C8	2.480(13)
Li1−C4	2.920(15)	Li2−C9	2.307(12)
		Li2−Cp2	2.144(15)
C27−C28	1.524(5)	C10−C27	1.569(7)
Li1−N4	2.179(10)	Li2−N3	2.546(10)
Li−H1−Li2	156		
Zr1−H1−Li2	102		
Zr1−H1−Li1	98		

[a] Cp2 and Cp4 refer to the centroids of the pyrrole rings containing N2 and N4, respectively.

conformation; Zr and C5 are displaced by 1.069(1) Å and 0.765(4) Å, respectively, from the N1,N2,C4,C6 plane on the same side. We also wish to underline the role of the alkali metals in modeling the conformation of the molecule: the two adjacent pyrrole rings, which are bent as a consequence of metalation, do not show any twisting in the presence of potassium in **5** while they are significantly twisted in the presence of lithium in **2**. In complex **2** the twisting can be deduced from the nonplanarity of the group of atoms N2,N3,-C9,C11 with displacements of atoms from the least squares plane ranging from −0.141(5) to 0.077(4) Å; zirconium and C10 are 0.724(1) and 0.645(5) Å from this mean plane. The trans dimetalation both in **5** and **6** results in a bending of the molecule along the line through the C5···C5′ *meso* carbons. The two symmetry-related N1-C1···C4,C10′,N2′-C6′···C9′ and N1′-C1···C4′,C10,N2-C6···C9 moieties are approximately planar (maximum distortion 0.101(4) Å for C8), the least-squares mean planes through them forming a dihedral angle of 106.2(1) Å. The out-of-plane distances of the Zr,C5,C5′ atoms from these planes are −0.226(1), −0.190(4), 0.072(4) Å. The bending favors η^5-interactions between two facing pyrrole rings and the potassium cations.

The isolation of the mixture of **5** + **6** did not clarify the genesis of the side chain metalation and the relationship between **4** and **5** + **6**. To this purpose we performed a number of experiments. We found that the isomeric **5** vs **6** ratio remains the same when we heat **4** in the presence of excess KH under the conditions of reaction 6. The result outlined above can be accounted for if the zirconium−carbon bond exchanges easily in an intramolecular fashion with the C−H bonds of other side chains of the porphyrinogen ligand. In particular, this can account for the transformation of **4**, metalated exclusively at the *β*-carbon of the ethyl group, into the mixture of **5** and **6**, metalated at the α and *β* carbons of the ethyl group, respectively. This form of *σ*-bond metathesis of Zr−C and C−H bonds has much precedent in high-valent early transition and lanthanide metals.[2]

$$L_nZrR + R'H \rightarrow L_nZrR' + RH \qquad (7)$$

Reactivity of the Metalated Forms. The Zr−C bonds made via the intramolecular metalation of the porphyrinogen periphery should allow its easy functionalization using conventional organometallic methodologies. Among the reactions that have been explored, we report the insertion of isocyanides and carbon monoxide.

The reaction of **2** with Bu^{t}NC in toluene occurred with its insertion into the Zr−C bond and the formation of an η^2-iminoacyl,[13] while the triply bridged hydride remains unchanged.

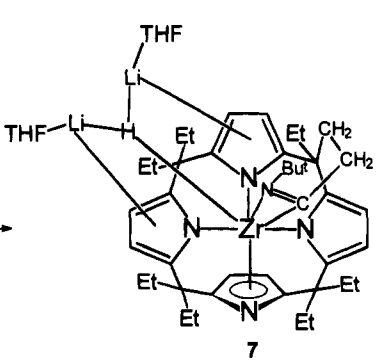

2 + ButNC ⟶ **7** (8)

(13) Iminoacyl formed from migratory insertion of RNC with M−C bonds is a well-known reaction: Singleton, E.; Ossthnizen, H. E. *Adv. Organomet. Chem.* **1983**, *22*, 209. Otsuka, S.; Nakamura, A.; Yoshida,T.; Naruto, M.; Ataba, K. *J. Am. Chem. Soc.* **1973**, *95*, 3180. Yamamoto, Y.; Yamazaki, H. *Inorg. Chem.* **1974**, *13*, 438. Aoki, K.; Yamamoto, Y. *Inorg. Chem.* **1976**, *15*, 48. Bellachioma, G.; Cardaci, G.; Zanazzi, P. *Inorg. Chem.* **1987**, *26*, 84. Maitlis, P. M.; Espinet, P.; Russell, M. J. H. In *Comprehensive Organometallic Chemistry*; Wilkinson, G., Stone, F. G. A., Abel, E. W., Eds.; Pergamon: London, 1982; Vol. 8., Chapter 38.4. Crociani, B. In *Reactions of Coordinated Ligands*; Braterman, P. S., Ed.; Plenum: New York, 1986; Chapter 9.

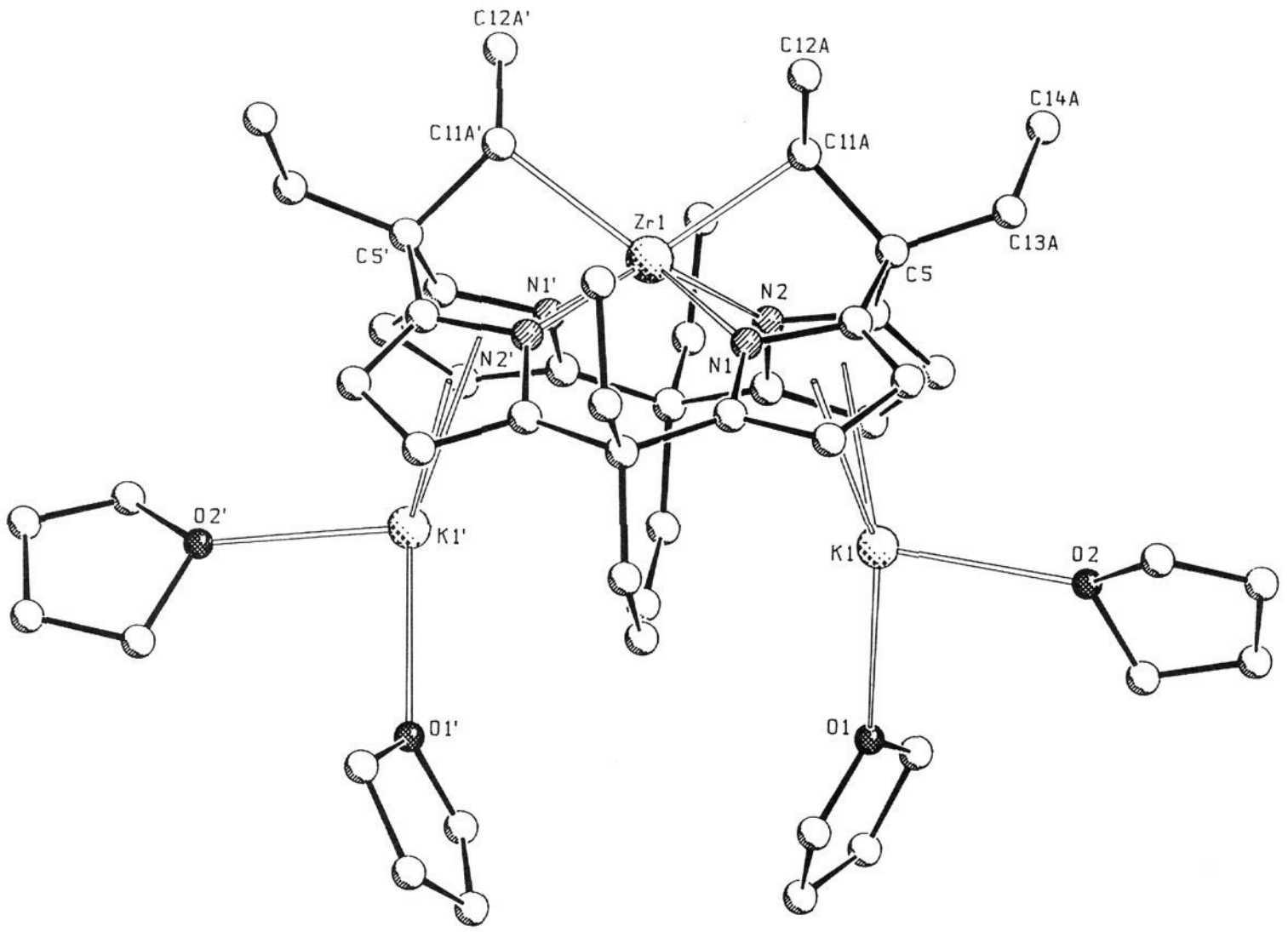

Figure 2. SCHAKAL drawing of α-metalated isomer of complex **5**. Prime denotes a transformation of -*x*, y, $^1/_2 - z$.

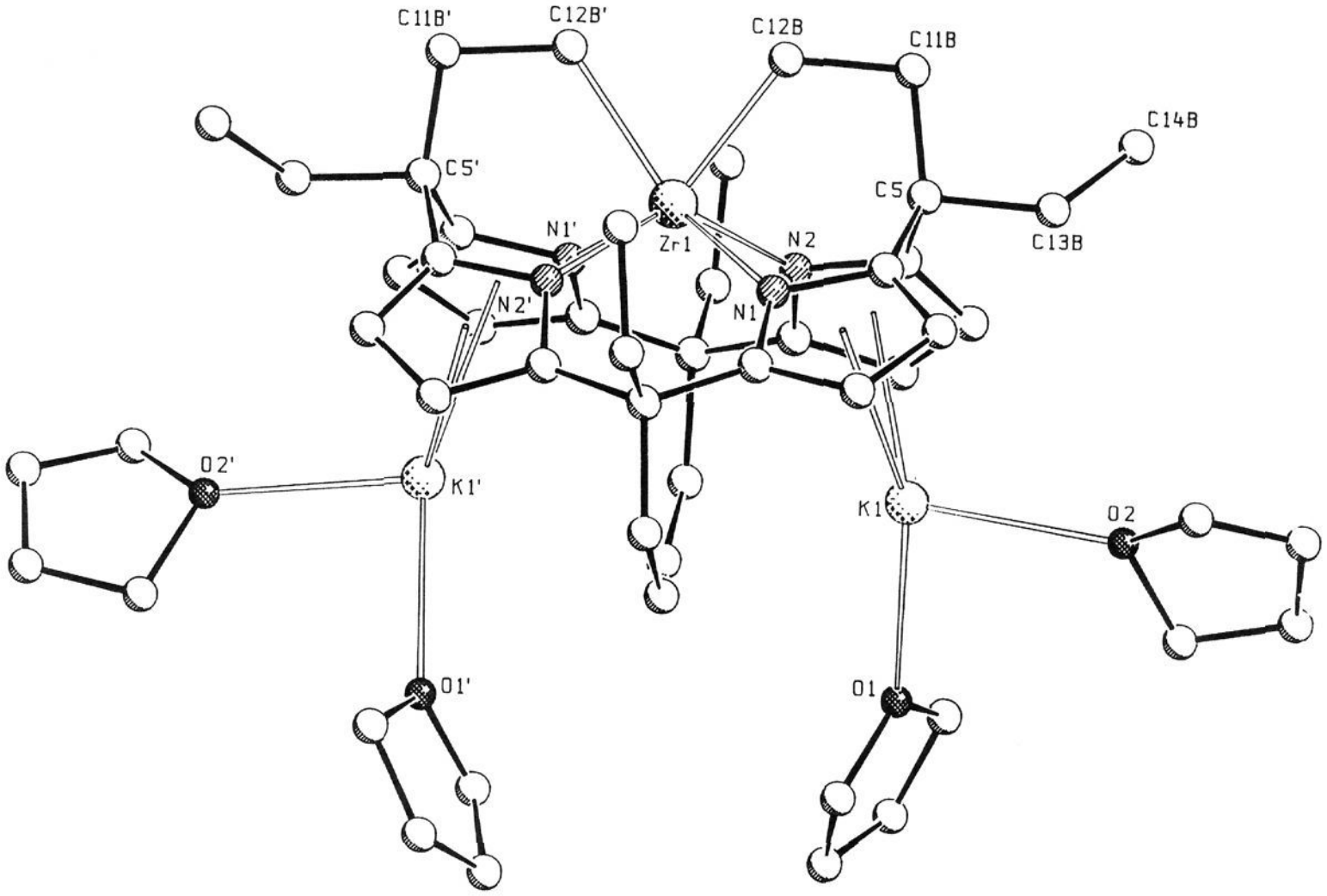

Figure 3. SCHAKAL drawing of β-metalated isomer of complex **6**. Prime denotes a transformation of $-x$, y, $^1/_2 - z$.

Although the IR (ν_{CN} = 1674 cm^{-1}), NMR, and other analytical data for **7** are in agreement with the proposed structure, an X-ray structural analysis was performed to confirm this structure.

Complex **7**, in which the porphyrinogen exhibits an η^5-η^1-η^1-η^1 bonding mode, is shown in Figure 4. Selected interatomic distances are listed in Table 4 with relevant conformational parameters compared in Table 7. The η^2-iminoacyl shows the usual structural parameters with a N5−C37 bond distance of 1.268(4) Å. Metalation and insertion cause a remarkable puckering of the two adjacent N1···N2 and N2···N3 six-membered chelation rings. The N1···N2 six-membered ring is twisted with respect to the Zr−C5 line, the dihedral angle between the opposite N1−C4 and N2−C6 bonds being 45.9(2)°. The N2···N3 ring assumes a half-boat distorted conformation, the zirconium atom protruding by 1.278(1) Å from the mean

Table 3. Selected Interatomic Distances (Å) and Angles (deg) for Complex **5** + **6**[a,b]

complex **5**		complex **6**	
Zr1−N1	2.198(3)	Zr1−N2	2.196(2)
Zr1−C11A	2.338(6)	Zr1−C12B	2.226(17)
K1−O1	2.708(4)	K1−O2	2.719(5)
K1−N1	3.246(3)	K1−N2	3.451(3)
K1−C1	3.409(4)	K1−C6	3.081(4)
K1−C2	3.281(4)	K1−C7	3.024(4)
K1−C3	3.041(4)	K1−C8	3.371(4)
K1−C4	3.010(4)	K1−C9	3.618(3)
K1−Cp1	2.975(4)	K1−Cp2	3.100(4)
N1−C1	1.377(5)	N2−C6	1.376(4)
N1−C4	1.386(4)	N2−C9	1.382(4)
C1−C2	1.381(4)	C6−C7	1.369(5)
C2−C3	1.406(6)	C7−C8	1.418(5)
C3−C4	1.381(4)	C8−C9	1.377(5)
C4−C5	1.509(6)	C9−C10	1.517(4)
C1−C10′	1.508(6)	C5−C6	1.521(5)
C5−C11A	1.614(7)	C5−C11B	1.495(11)
C5−C13A	1.552(8)	C5−C13B	1.560(15)
C11A−C12A	1.545(8)	C11B−C12B	1.528(22)
C13A−C14A	1.543(11)	C13B−C14B	1.547(23)
C11A−Zr1−C11A′	108.9(2)	C12B−Zr1−C12B′	73.4(6)
N1−Zr1−N2	85.6(1)	N1−Zr1−N1′	134.4(1)
N1−Zr1−N2′	77.1(1)	N2−Zr1−N2′	134.5(1)
N1−K1−C1	23.7(1)	N2−K1−C6	23.4(1)
N1−K1−C4	25.2(1)	N2−K1−C9	22.4(1)
C1−K1−C2	23.7(1)	C6−K1−C7	25.9(1)
C2−K1−C3	25.3(1)	C7−K1−C8	24.9(1)
C3−K1−C4	26.4(1)	C8−K1−C9	22.3(1)
O1−K1−O2	90.6(1)		
Zr1−N1−C4	113.7(2)	Zr1−N2−C9	136.5(2)
Zr1−N1−C1	137.9(2)	Zr1−N2−C6	114.1(2)
C1−N1−C4	108.4(3)	C6−N2−C9	107.9(2)

[a] ′ = −*x*, *y*, 0.5 − *z*. [b] Cp1 and Cp2 refer to the centroids of the pyrrole rings containing N1 and N2, respectively.

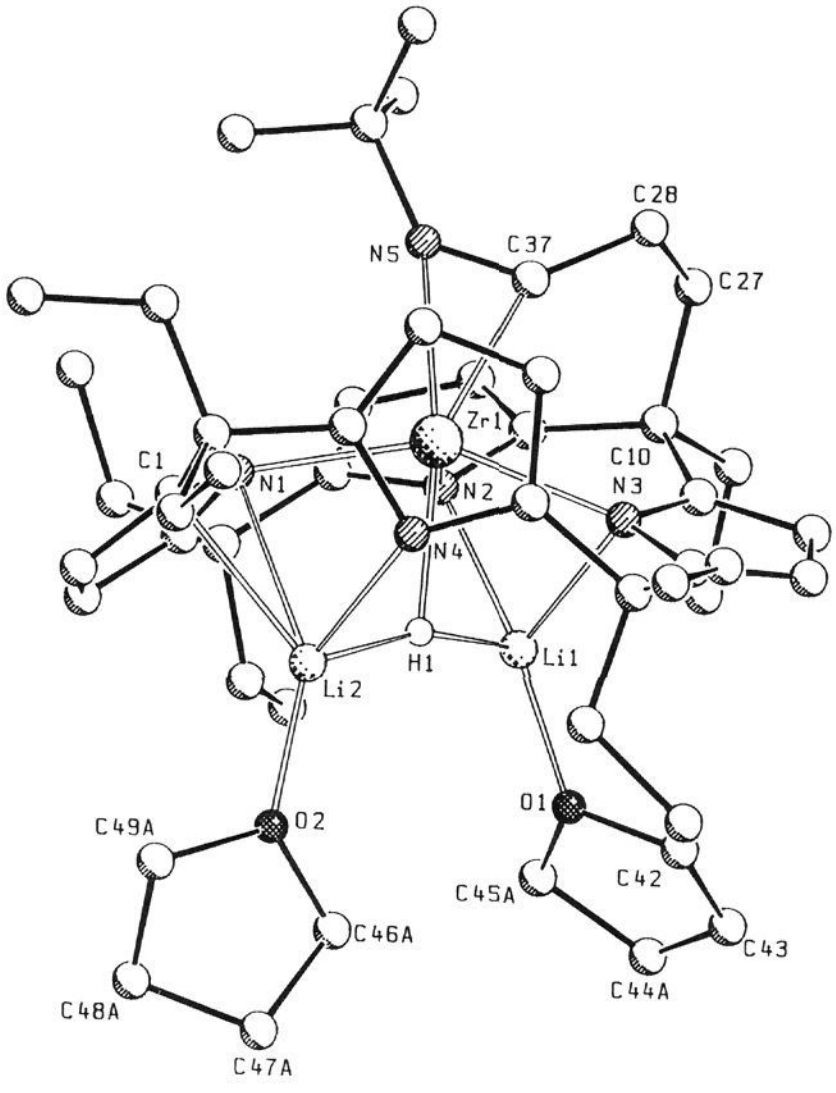

Figure 4. SCHAKAL drawing of complex **7**. Disorder omitted for clarity.

least-squares plane running through the N2,C9,C10,C11,N3 atoms. The rest of the structure is similar to that of its precursor, **2**, with the following differences believed to arise from the presence of the bulky inserted molecule: (i) a small, yet significant, lengthening of the Zr−N(1−4) bond distances [average value 2.281(3) Å *vs* 2.238(10) Å]; (ii) tetrahedral distortions of the N_4 core accompanied by a substantial displacement of the Zr atom out of the N_4 plane and from the A and B pyrrole plane (Table 7). The structural parameters of the [Li_2H] moiety resemble closely those in **2**.

Table 4. Selected Interatomic Distances (Å) and Angles (deg) for Complex **7**

Zr1−N1	2.276(2)	Zr1−C17	2.588(4)
Zr1−N2	2.283(2)	Zr1−C18	2.634(4)
Zr1−N3	2.284(2)	Zr1−C19	2.516(4)
Zr1−N4	2.447(2)	Zr1−C37	2.199(4)
Zr1−N5	2.297(2)	Zr1−Cp4	2.237(4)
Zr1−C16	2.480(4)		
Li1−O1	1.899(8)	Li2−N1	2.557(10)
Li1−N2	2.098(8)	Li2−N4	2.145(8)
Li1−N3	2.198(6)	Li2−C1	2.388(11)
Li2−O2	1.895(10)		
N5−C37	1.268(4)	C10−C27	1.572(6)
N5−C38	1.498(6)	C19−C20	1.528(5)
C27−C28	1.534(6)	C28−C37	1.511(5)
N1−Li2−N4	82.6(3)	Zr1−N5−C38	159.8(2)
O2−Li2−C1	127.8(4)	Zr1−N5−C37	69.4(2)
O2−Li2−N4	129.5(5)	C37−N5−C38	130.5(3)
O2−Li2−N1	145.2(4)		
C10−C27−C28	116.8(3)	Zr1−C37−C28	145.2(3)
C27−C28−C37	110.6(3)	Zr1−C37−N5	77.9(2)
N5−C37−C28	136.8(3)		

A useful functionalization of the Zr−C bond via insertion reactions requires that we must be able to remove the final functionality from the metal. The reactivity of η^2-acyls and η^2-iminoacyls is sometimes more intriguing than expected,[11a,13] and the assistance of the metal can lead to some unexpected results, as in the present case where we formed novel macrocyclic structures.

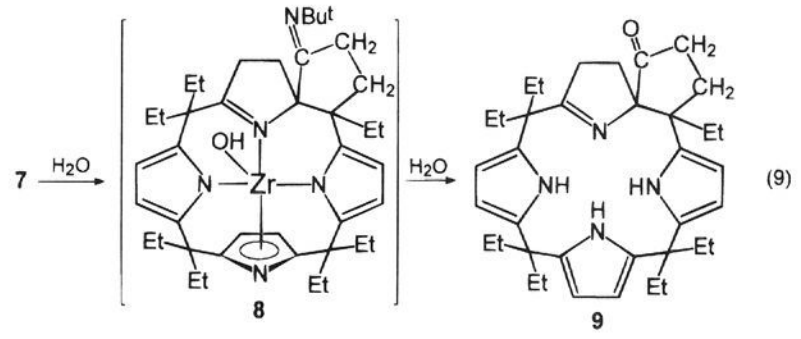

The hydrolysis of **7** in H_2O leads to **9** via the plausible intermediacy of **8**. The genesis of **8** and **9** is accounted for by the carbenium ion nature of the carbon in the η^2-iminoacyl[14] promoting attack upon the electron-rich pyrrolyl anion in the α-position during the preliminary stage of the hydrolysis. Furthermore, we found that the same pyrrole underwent hydrogenation of one of its C=C double bonds from the dihydrogen formed upon the protolysis of the hydride ligand in **7**. The nature of **9** has been elucidated by conventional spectroscopic methods and also by an X-ray analysis.[15] The intermediacy of **8** was supported by the isolation of an analog

(14) Tatsumi, K.; Nakamura, A.; Hofmann, P.; Stauffert, P.; Hoffmann, R. *J. Am. Chem. Soc.* **1985**, *107*, 4440. Martin, B. D.; Matchett, S. A.; Norton, J. R.; Anderson, O. P. *J. Am. Chem. Soc.* **1985**, *107*, 7952. Fanwick, P. E.; Kobriger, L. M.; McMullen, A. K.; Rothwell, I. P. *J. Am. Chem. Soc.* **1986**, *108*, 8095. Arnold, J.; Tilley, T. D.; Rheingold, A. L. *J. Am. Chem. Soc.* **1986**, *108*, 5355. Roddick, D. M.; Bercaw, J. E. *Chem. Ber.* **1989**, *122*, 1579. Hofmann, P.; Stauffert, P.; Frede, M.; Tatsumi, K. *Chem. Ber.* **1989**, *122*, 1559. Hofmann, P.; Stauffert, P.; Tatsumi, K.; Nakamura, A.; Hoffmann, R. *Organometallics* **1985**, *4*, 404. Tatsumi, K.; Nakamura, A.; Hofmann, P.; Hoffmann, R.; Moloy, K. G.; Marks, T. J. *J. Am. Chem. Soc.* **1986**, *108*, 4467.

(15) Jacoby, D.; Isoz, S.; Floriani, C.; Chiesi-Villa, A.; Rizzoli, C. Unpublished results.

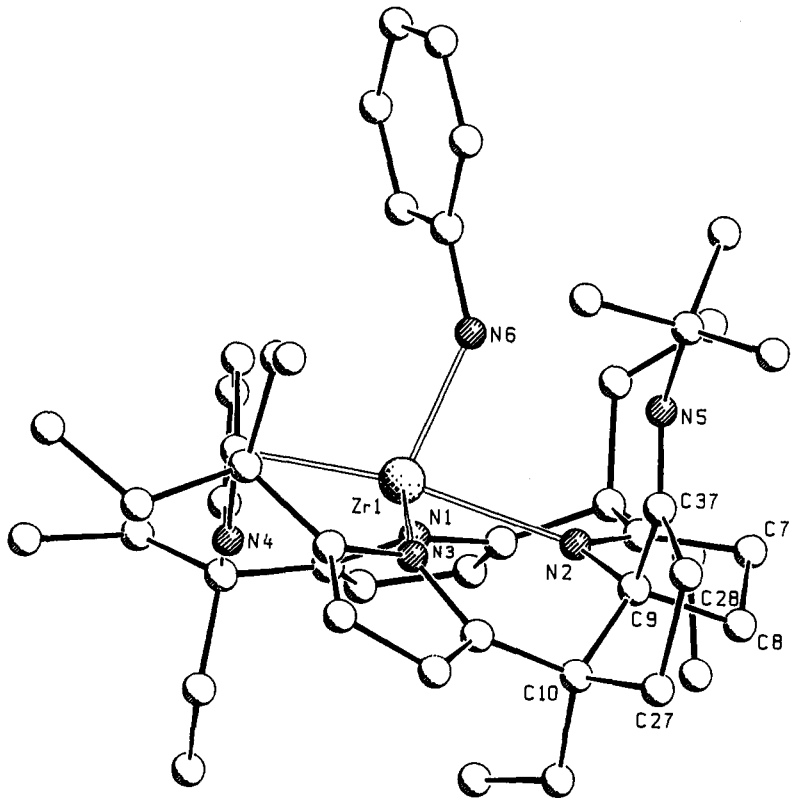

Figure 5. SCHAKAL drawing of complex **10**.

of **8** that was obtained under controlled hydrolysis of **7**. In fact, when the protolysis of **7** was carried out in aprotic solvents using $PhNH_2$·HCl in a 2:1 molar ratio, **10** was isolated. The protonation of the η^2-imino group enhances its carbenium ion reactivity,[14] thus promoting its attacking the α-position of an adjacent pyrrole ring.

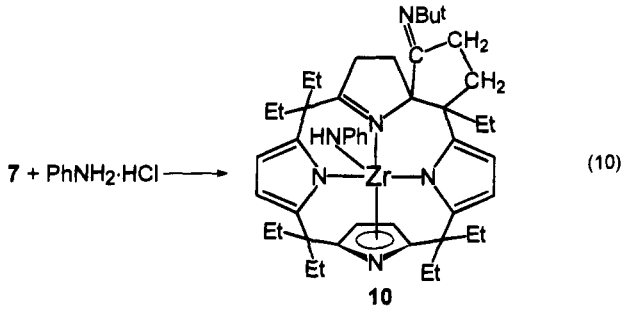

(10)

The resulting modification of the macrocyclic ligand has been elucidated by an X-ray analysis, which supports the picture shown for **10**. The original porphyrinogen tetraanion has been converted into a trianionic macrocycle, where one of the pyrrolyl anions becomes a dihydropyrrolidine fragment. The crystal structure of **10** is shown in Figure 5. Selected bond distances and angles are listed in Table 5 with the relevant conformational parameters given in Table 7. The trianionic porphyrinogen-type ligand exhibits a η^5-η^1-η^1-η^1 bonding mode and shows some main features: (i) the cyclopentane ring having an envelope conformation. The C37 carbon maintains an sp^2 hybridization state, the value of the N5−C37 distance being 1.248(14) Å; (ii) the presence of C7−C8 single bond and the localization of a double bond in the B pyrrole ring [N2−C6, 1.319(10) Å, C6−C7, 1.503(14) Å]; (iii) the Zr−N bond distances involving the σ-bonded pyrrole rings affected by the different charge of the anion, the Zr−N2 bond distance [2.356(7) Å] being markedly elongated.

The Zr−N6 bond distance [2.058(7) Å] in **10** is in good agreement with those found in other zirconium amido derivatives,[16] *e.g.*, in $[(\mu\text{-N-Bu}^t)\text{Zr}(\text{NMe}_2)]_2$. The direction of this bond is tilted by 24.2(2)° with respect to the normal to the N_4 plane. This deformation which is present also in the metalated and alkylated complexes could be attributed to a steric hindrance involving the η^5-bonded pyrrole ring [minimum contact distance N6···C17, 3.005(12) Å]. The two adjacent N1···N2 and N2···N3 six-membered chelation rings are distinctly puckered. The N1···N2 ring has a boat conformation, zirconium and C5 lying 0.795(1) and 0.410(8) Å from the plane through the N1,-C4,C6,N2 atoms. The N2···N3 ring is twisted along the Zr···C10 line, as indicated by the dihedral angle between the direction of the N2−C9 and N3−C11 bonds [31.1(5)°].

Table 5. Selected Bond Distances (Å) for Complex **10**

Zr1−N1	2.189(6)	Zr1−C16	2.423(8)
Zr1−N2	2.356(7)	Zr1−C17	2.624(9)
Zr1−N3	2.195(7)	Zr1−C18	2.644(9)
Zr1−N4	2.375(6)	Zr1−C19	2.497(8)
Zr1−N6	2.058(7)	Zr1−Cp4	2.212(8)
N2−C6	1.319(10)	N5−C37	1.248(14)
N2−C9	1.489(12)	N5−C38	1.489(12)
N6−C51	1.398(13)	C10−C27	1.585(13)
C9−C37	1.531(12)	C27−C28	1.561(14)
C10−C11	1.510(12)	C28−C37	1.550(15)

The isolation of **9** and **10** further sheds light on the previously reported homologation[17] of a pyrrole to pyridine within the porphyrinogen skeleton.[4a,18] Such a reaction occurs via the migratory insertion of carbon monoxide into Zr−H and Zr−C bonds, established via the addition of alkali hydrides and alkali

(16) Brubaker, G. R.; Jarke, F. H.; Brubaker, I. N. *Inorg. Chem.* **1979**, *18*, 2030.

(17) For a general review on the homologation reaction of alcohols and related species, see: Chiusoli, G. P.; Salerno, G.; Foa, M. In *Reactions of Coordinated Ligands*; Braterman, P. S., Ed.; Plenum: New York, 1986; Vol. 1, Chapter 7. Parshall, G. W.; Ittel, S. D. *Homogeneous Catalysis*, 2nd ed.; Wiley: New York, 1992. Colquhoun, H. M.; Thompson, D. J.; Twigg, M. V. *Carbonylation*; Plenum: New York, 1991.

(18) Jacoby, D.; Isoz, S.; Floriani, C.; Chiesi-Villa, A.; Rizzoli, C. *J. Am. Chem. Soc.* **1995**, *117*, 2793.

alkyls to **1**, followed by the reaction of the resulting η^2-acyl carbenium ion on the pyrrole ring. Compounds **9** and **10** are the plausible intermediates preceding the homologation of the pyrrole to pyridine within the porphyrinogen skeleton. They result from an attack of the protonated η^2-iminoacyl having carbenium ion properties on the α-position of the pyrrole. The reaction does not, however, proceed further because in such cases we do not have any driving force derived from the oxophilicity of the metal toward the η^2-acyl. In fact, when **2** was reacted with CO or a source of CO instead of Bu^{t}NC we achieved the homologation of a pyrrole ring. The reaction of **2** with carbon monoxide or $Mo(CO)_6$, which functions as a convenient source of low concentration levels of carbon monoxide, led to the isolation of **11**.

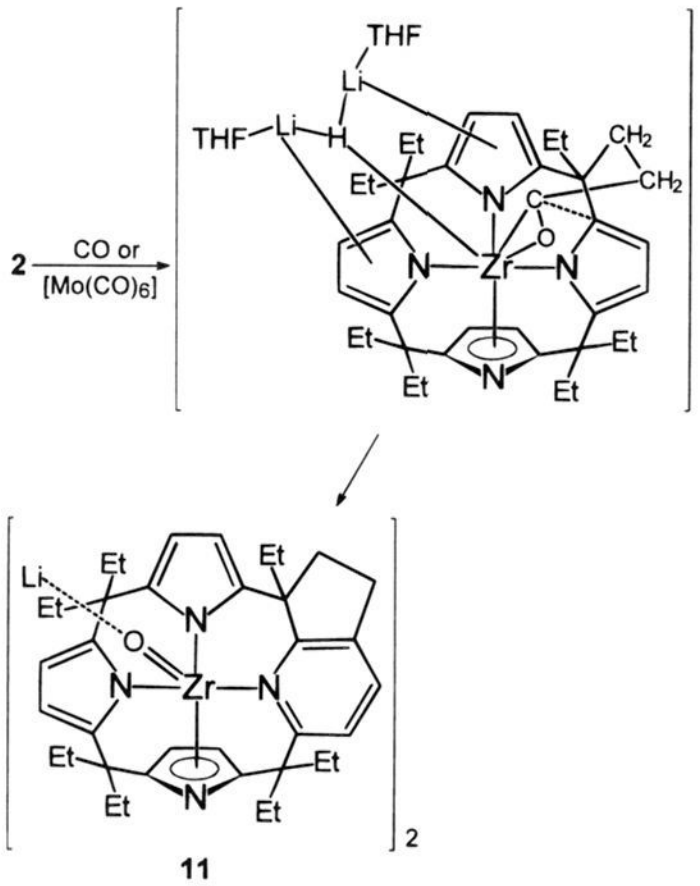

(11)

The structure of **11** (*vide infra*) shows that the migratory insertion of CO into the Zr−C bond of the metalated form **2** of the porphyrinogen proceeds with the intermediate formation of a carbenium η^2-acyl derivative,[14] which attacks one of the electron-rich pyrrole rings, as supported by the isolation of analogous compounds **9** and **10**. This is followed by the ring opening of the pyrrole, leading to a *meta*-substituted pyridine and the cleavage of the C−O bond.[4b,18] Such a cleavage produces a zirconyl compound ($\nu_{Zr=O}$, 776 cm^{-1})[4b,18,19] in the form of a dimer where the two monomeric units are bridged by two lithium cations. The Li−H unit present in **2** has been removed during the reaction with both CO and $[Mo(CO)_6]$, though we did not find under which form.

The structure of **11** is depicted in Figures 6A and 6B. It consists of centrosymmetric dimers (Figure 6B) and toluene solvent molecules in a complex/toluene ratio of 1/1.2 established by the X-ray analysis (see Experimental Section). Selected bond distances and angles are listed in Table 6. Figure 6A shows an ORTEP projection of the zirconyl unit. The most relevant conformational parameters are compared in Table 7. The Zr−O distance [1.838(7) Å] is consistent with the existence of a Zr−O double bond.[4b,18,19] Each independent lithium cation shows an η^5-interaction with the B pyrrole ring (Table 7) and bridges two symmetry-related zirconyl units through the oxygen atoms, giving rise to the dimer.

(19) Another kind of zirconyl compounds, namely $[(\eta^5\text{-}C_5Me_5)_2ZrO(Py)]$ [ν(Zr=O), 780 cm^{-1}], has been recently reported: Howard, W. A.; Waters, M.; Parkin, G. *J. Am. Chem. Soc.* **1993**, *115*, 4917.

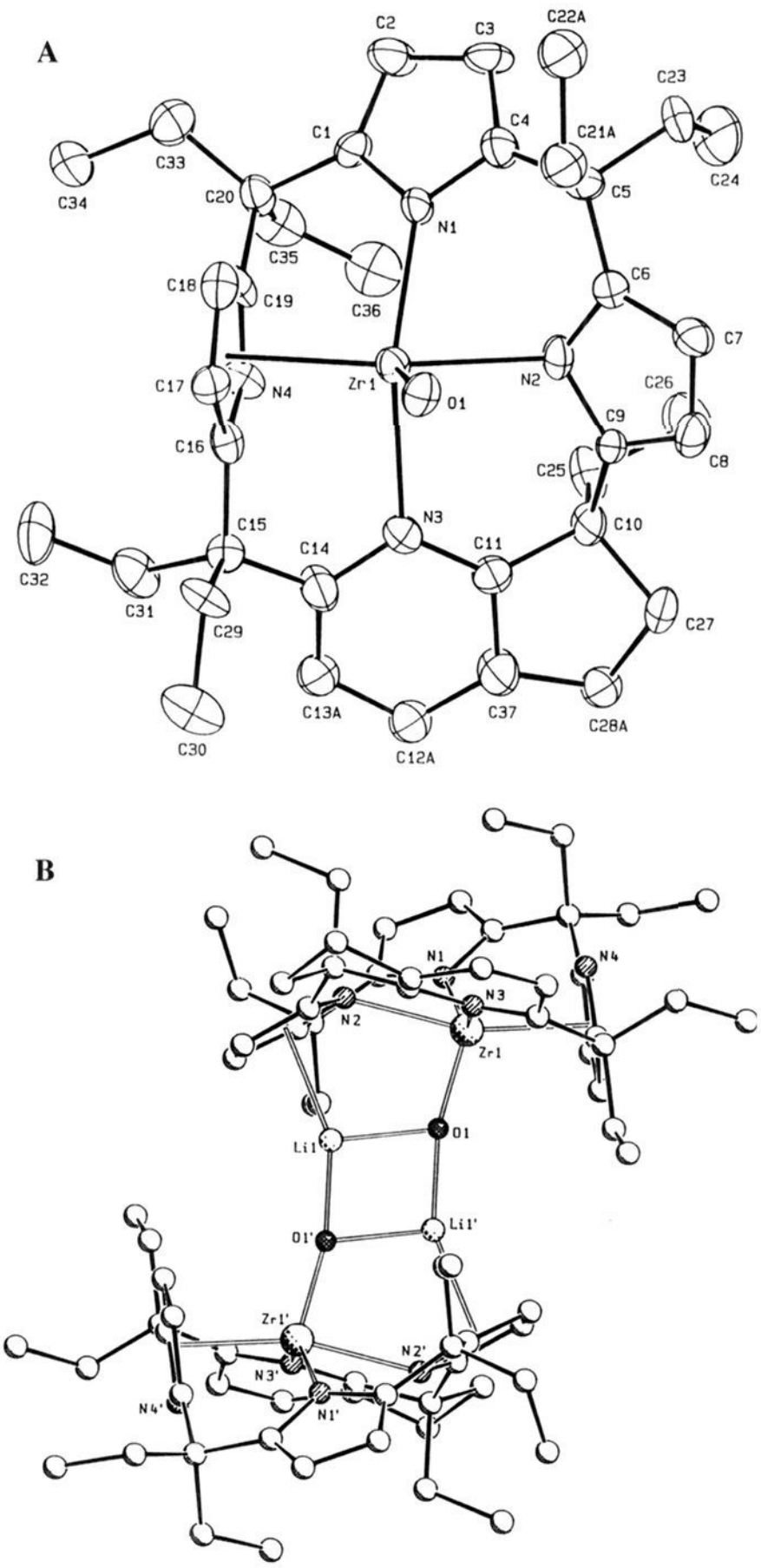

Figure 6. (A) ORTEP drawing of the anion in complex **11** (30% probability ellipsoids). Disorder omitted for clarity. (B) SCHAKAL drawing of the dimer (complex **11**). Disorder omitted for clarity.

The trispyrrole−monopyridine ligand is η^5-η^1-η^1-η^1-bonded to zirconium, with the pyridine interacting at a rather long distance [2.444(9) Å].[4b,18] The N_4 core shows the usual tetrahedral distortion, zirconium protruding by 0.799(1) Å toward the oxygen atom. The direction of the Zr−O bond forms a dihedral angle of 25.3(3)° with the normal to the N_4 core, as before, away from the η^5-pyrrole. The bending of the pyrrole rings around the N_4 core is described by the dihedral angles given in Table 7, indicating a very distorted conformation. In addition the adjacent N1···N2 and N2···N3 six-membered chelation rings are twisted along the Zr···C5 and Zr···C10 lines as indicated by the dihedral angles between the lines N1−C4, N2−C6 [29.3(8)°] and N2-C9, N3-C11 [37.7(8)°].

Conclusions

The metalation of aliphatic chains at the periphery of *meso*-octaethylporphyrinogen has been achieved via the electrophilic

Table 6. Selected Bond Distances (Å) and Angles (deg) for Complex **11**[a]

Zr1−O1	1.838(7)	Zr1−C16	2.498(12)
Zr1−N1	2.217(9)	Zr1−C17	2.623(12)
Zr1−N2	2.274(9)	Zr1−C18	2.609(12)
Zr1−N3	2.478(12)	Zr1−C19	2.496(12)
Zr1−N4	2.444(9)	Zr1−Cp4	2.244(11)
Li1−O1	1.992(20)	Li1−C7	2.363(27)
Li1−O1′	1.817(22)	Li1−C8	2.399(27)
Li1−N2	2.570(22)	Li1−C9	2.543(25)
Li1−C6	2.486(25)		
N3−C11	1.381(16)		
N3−C14	1.347(18)		
C11−C37	1.386(21)	C12A−C13A	1.43(4)
C12A−C37	1.44(4)	C13A−C14	1.44(4)
C14−C15	1.445(18)	C15−C16	1.528(18)
C10−C11	1.491(20)	C27−C28A	1.693(34)
C10−C27	1.524(18)	C28A−C37	1.545(31)
Zr1−O1−Li1	111.9(7)	Zr1−O1−Li1′	166.5(8)
Li1−O1−Li1′	80.4(9)		

[a] ′ = −x, −y, −z.

activation of the C−H bond followed by the removal of the β-proton using alkali hydrides. The success of such a class of reactions depends (i) on the bifunctional nature of metal−porphyrinogen complexes which possess the ability to bind cations at the electron-rich periphery and thus to function as polar organometallic carriers and (ii) on the appropriate conformations of the porphyrinogen allowing the C−H bond of the periphery to come into very close proximity to the central electrophilic metal. An intramolecular σ-bond metathesis between Zr−C and C−H bonds was observed in the conversion of β- to α-metalated forms of the ethyl groups of porphyrinogen. The migratory insertion of Bu^{t}NC and carbon monoxide into the Zr−C bond allowed the introduction of functionalities at the periphery of the porphyrinogen and the attainment of novel forms of porphyrinogen. In particular, the insertion of Bu^{t}NC into the Zr−C bond of the monometalated form **2** allowed us to isolate the corresponding η^2-iminoacyl. Its carbenium ion properties were exemplified when it underwent hydrolysis reactions. The electrophilic carbenoid species attacks the α-carbon of a pyrrole leading to a functionalized five-membered ring. This complex can be considered as a model intermediate in the homologation of pyrrole to pyridine in the reaction with carbon monoxide. Further, the reaction of **2** with CO led directly to the homologation of one of the pyrrole rings, thus in **11** a pyrrole ring has been converted to a pyridine with a fused cyclopentene ring. The results we have reported emphasize how appropriate organometallic methodologies (bifunctional complexes, conformational effects, polar organometallic carriers) allow the activation and functionalization of aliphatic substituents in large organic molecules.

Experimental Section

General Procedure. All reactions were carried out under a purified nitrogen atmosphere. Solvents were dried and distilled, by standard methods, before use. Infrared and ^{1}H NMR spectra were recorded with a Perkin-Elmer 1600 FT-IR spectrophotometer and either a 200-AC or an ARX-400 Bruker instrument, respectively. The synthesis of **1** was performed as reported.[4a]

Preparation of 2. THF (2.5 mL, 30.8 mmol) was added to a toluene (200 mL) solution of **1** (19.63 g, 28.04 mmol), to which was then added solid LiH (1.67 g, 209.6 mmol). The suspension was heated at 100 °C for 3 days under partial vacuum. The yellow solution was filtered to remove the excess solid LiH. The solution was evaporated to dryness and the solid residue was collected with *n*-hexane (15.50 g, 70%). Anal. Calcd for $C_{44}H_{64}Li_2N_4O_2Zr$: C, 67.21; H, 8.22; N, 7.13. Found: C, 66.77; H, 8.24; N, 7.15. ^{1}H NMR (200 MHz, C_6D_6, room temperature): δ 0.6−1.1 (m, 21 H, CH_3); 1.15 (m, 8 H, THF); 1.47 (t, 2 H, ^3J = 7.3 Hz, CH_2−Zr); 1.75−2.7 (m, 16 H, CH_2); 3.11 (m, 8 H, THF); 5.9−6.7(m, 8 H, CH).

In order to investigate possible transformations of **2** the following two experiments have been performed: (a) **2** (1.60 g) was heated in refluxing THF for 4 days; (b) **2** (1.60 g) was heated in refluxing THF for 5 days in the presence of LiH (0.70 g, 40.0 mmol). In both cases the starting material was recovered unchanged.

Preparation of 3. NaH (1.12 g, 46.66 mmol) was added to a THF (100 mL) solution of **1** (10.92 g, 15.59 mmol). The suspension was kept at 70° C for 2 days under partial vacuum. The excess of NaH was removed by filtration, and then the solvent was reduced to 20 mL. Toluene (200 mL) was added to the suspension, which was heated until a solution was obtained. Small amounts of a white solid were obtained on cooling and these were removed by filtration. The resulting solution was evaporated to 15 mL, and 50 mL of *n*-hexane was added. Cooling to −20 °C gave yellow crystals of **3** (5.95 g, 46%). Crystals suitable for an X-ray analysis were obtained by recrystallization from an *n*-hexane/THF mixture. Anal. Calcd for $C_{44}H_{64}N_4Na_2O_2Zr$: C, 64.57; H, 7.90; N, 6.85. Found: C, 64.98; H, 8.34; N, 6.39. ^{1}H NMR (200 MHz, C_6D_6, room temperature): δ 0.03 (m, 1 H, H-Zr); 0.75−1.10 (m, 18 H, CH_3); 1.30 (m, 8 H, THF); 1.45 (t, 3 H, CH_3); 1.7−3.0 (m, 18 H, CH_2); 3.30 (m, 8 H, THF); 5.98 (s, 2 H, CH); 6.06 (d, 1 H, J = 2.7 Hz, CH); 6.12 (d, 1 H, J = 3.2 Hz, CH); 6.13 (s, 2 H, CH); 6.84 (d, 1 H, J = 2.6 Hz, CH); 7.08 (d, 1 H, J = 2.7 Hz, CH).

Preparation of 4. A THF (30 mL) solution of **2** (1.30 g, 1.65 mmol) was heated at 50 °C in the presence of KH (0.23 g, 5.75 mmol) for 24 h. The excess KH and the LiH formed during the reaction were filtered out. The yellow solution was evaporated to 15 mL and gave crystals of **4** (0.90 g, 64%). Anal. Calcd for $C_{44}H_{64}K_2N_4O_2Zr$: C, 62.19; H, 7.54; N, 6.60. Found: C, 61.75; H, 7.72; N, 6.54. ^{1}H NMR (200 MHz, C_4D_8O, room temperature): δ −0.93 (m, 1 H, H); 0.27 (t, 3 H, CH_3); 0.56 (m, 2 H, CH_2−Zr); 0.74 (t, 3 H, CH_3); 0.77 (m, 12 H,

Table 7. Comparison of Structural Parameters for compounds **2**, **5** + **6**, **7**, **10**, and **11**

		2	**5** + **6**[b]	**7**	**10**	**11**[c]
dist of atoms from N4 core, Å	N1	0.036(4)	−0.002(4)	0.071(2)	−0.027(6)	0.063(9)
	N2	−0.036(4)	0.002(4)	−0.078(2)	0.033(6)	−0.068(9)
	N3	0.031(4)	−0.002(4)	0.070(2)	−0.033(6)	0.087(11)
	N4	−0.030(4)	0.002(4)	−0.063(2)	0.029(6)	−0.074(10)
	Zr	0.593(1)	0.851(1)	0.699(1)	0.801(1)	0.799(1)
dist of Zr from A, Å[a]		0.836(1)	0.037(1)	1.040(1)	0.215(1)	0.207(1)
dist of Zr from B, Å[a]		1.080(1)	0.413(1)	1.560(1)	0.189(1)	1.515(1)
dist of Zr from C, Å[a]		0.459(1)	0.037(1)	0.520(1)	0.405(1)	0.093(1)
dist of Zr from D, Å[a]		2.234(1)	0.413(1)	2.228(1)	2.190(1)	2.236(1)
dihedral angles between the N4 core	(A)	137.9(1)	145.6(3)	133.6(1)	160.6(2)	151.0(3)
and the A,B,C,D rings, deg	(B)	130.6(1)	138.7(3)	151.4(1)	156.9(3)	24.0(3)
	(C)	164.6(1)	145.6(3)	166.3(1)	137.1(2)	154.5(4)
	(D)	82.2(1)	138.7(3)	84.8(1)	87.3(2)	88.9(3)
dihedral angles between AC		53.8(2)	68.8(1)	55.8(1)	61.5(3)	53.9(5)
dihedral angles between BD		53.6(3)	82.6(1)	63.0(1)	80.2(3)	69.6(4)

[a] Perpendicular distance of Zr from plane of pyrrole ring. A, B, C, and D define the pyrrole rings containing the N1, N2, N3, and N4 nitrogen atoms, respectively. [b] N3 and N4 should be read N1′ and N2′, respectively. [c] The values involving the disordered pyridine ring are referred to the A position.

CH_3); 1.07 (t, 3 H, CH_3); 1.40 (m, 4 H, CH_2); 1.68 (m, 8 H, THF); 1.65−2.20 (m, 14 H, CH_2); 3.58 (m, 8 H, THF); 5.35 (d, 1 H, J = 2.40 Hz, CH); 5.40 (d, J = 2.40 Hz, 1 H, CH); 5. 59 (s, 1 H, CH); 5.70 (d, J = 2.40 Hz, 1 H, CH); 5.84 (d, J = 2.40 Hz, 1 H, CH); 5.95 (s, 1 H, CH); 6.43 (d, J = 2.40 Hz, 1 H, CH); 6.95 (d, J = 2.40 Hz, 1 H, CH). The direct synthesis of **4** from **1** and KH is not practical. The reaction of **1** with KH gives a mixture of **4** and **5** + **6**.

Synthesis of 5 + 6, Method A. KH (2.20 g, 54.90 mmol) was added to a THF (100 mL) solution of **1** (10.89 g, 15.55 mmol). The suspension was kept at 70 °C for 6 days under vacuum, and then the solid was filtered out and the solvent completely evaporated. The yellow residue was collected using toluene (10.16 g, 66%). Crystals suitable for X-ray analysis were obtained by a recrystallization in an *n*-hexane/THF mixture. Anal. Calcd for $C_{52}H_{78}K_2N_4O_4Zr$: C, 62.91; H, 7.94; N, 5.64. Found: C, 62.23; H, 7.60; N, 6.18. ^{1}H NMR (200 MHz, THF-d_8, room temperature): δ 0.3 (m, 6 H, CH_3); 0.55 (m, 16 H, CH_3 + CH_2 + CH); 0.9 (m, 6 H, CH_3 + CH_2 + CH); 1.10 (m, 10 H, CH_3 + CH_2 + CH); 2.0 (m, 48 H, CH_2); 5.50−5.70 (m, 32 H, CH); 6.0 (m, 32 H, CH). If the reaction between **1** and KH is performed with a KH:**1** molar ratio lower than 3.5, then a mixture of **4** and **5** + **6** is obtained.

Synthesis of 5 + 6, Method B. Excess KH (0.23 g, 5.75 mmol) was added to a THF (30 mL) solution of **4** (1.00 g, 1.17 mmol). The suspension was refluxed for 3 days and became colorless. The KH excess was filtered out, and then the solvent was evaporated to dryness. The solid residue was recrystallized from THF/*n*-hexane, and a light yellow crystalline solid was obtained (0.20 g, 18%). This was shown to be the mixture **5** + **6** (analytical data as above).

Synthesis of 7. A toluene (120 mL) solution of **2** (8.42 g, 10.71 mmol) was stirred for 15 h at room temperature with Bu^{t}NC (1.3 mL, 0.96 g, 11.57 mmol). The light yellow solution was evaporated to dryness and the residue was collected using *n*-hexane (50 mL). The yellow powder was filtered and dried (5.68 g, 61%). Crystals suitable for an X-ray analysis were obtained by a recrystallization in *n*-hexane. Anal. Calcd for $C_{49}H_{73}Li_2N_5O_2Zr$: C, 67.69; H, 8.48; N, 8.06. Found: C, 67.82; H, 8.51; N, 8.14. IR, ν (cm^{-1}): 1647 (C=N). ^{1}H NMR (200 MHz, C_6D_6, room temperature): δ 0.59 (t, 3 H, ^3J = 7.3 Hz, CH_3); 0.84 (t, 3 H, CH_3); 0.87 (t, 3 H, CH_3); 0.90 (t, 3 H, CH_3); 1.04 (m, 8 H, THF); 1.19 (t, 6 H, CH_3); 1.25 (s, 9 H, Bu^t); 1.32 (t, 3 H, ^3J = 7.3 Hz, CH_3); 1.7−2.6 (m, 16 H, CH_2); 3.0 (m, 2 H, α-CH_2); 3.25 (m, 8 H, THF); 5.49 (d, 1 H, ^3J = 2.8 Hz, CH); 6.00 (d, 1 H, ^3J = 2.85 Hz, CH); 6.12 (d, 1 H, ^3J = 3.0 Hz, CH); 6.17 (d, 1 H, ^3J = 2.9 Hz, CH); 6.40 (d, 1 H, ^3J = 2.9 Hz, CH); 6.45 (t, 2 H, ^3J = 2.75 Hz, CH); 6.55 (d, 1 H, ^3J = 3.0 Hz, CH).

Synthesis of 9. Compound **7** (1.06 g, 1.22 mmol) was dissolved in toluene (25 mL) and hydrolyzed with H_2O (10 mL). After 1 night's stirring at room temperature, ZrO_2 was filtered off. The organic layer was separated and dried over Na_2SO_4, and then the solvent was evaporated to dryness and the beige powder (0.60 g, 87%) purified via silica gel chromatography using ethyl acetate:petroleum ether = 1:24 as eluant. The solvent was evaporated to dryness and the solid recrystallized from acetonitrile, affording white crystals (0.10 g). Anal. Calcd for $C_{37}H_{52}N_4O$: C, 78.11; H, 9.23; N, 9.85. Found: C, 77.93; H, 9.04; N, 9.44. IR, ν (cm^{-1}): 1747 (C=O); 3452 (NH); 3323 (NH). ^{1}H NMR (400 MHz, CD_2Cl_2, room temperature): δ 0.13 (t, 3 H, ^3J = 7.3 Hz, CH_3); 0.46 (t, 3 H, ^3J = 7.3 Hz, CH_3); 0.65−0.75 (m, 12 H, CH_3); 0,.82 (t, 3 H, ^3J = 7.4 Hz, CH_3); 1.15−1.30 (m, 2 H, CH_2); 1.4−2.4 (m, 18 H, CH_2); 2.55−2.75 (m, 2 H, CH_2); 5.75−5.80 (m, 3 H, CH); 6.00 (t, 1 H, ^3J = 3.2 Hz, CH); 6.03 (t, 1 H, ^3J = 3.0 Hz, CH); 6.21 (t, 1 H, ^3J = 3.1 Hz, CH); 7.04 (s, 1 H, NH); 7.37 (s, 1 H, NH); 10.49 (s, 1 H, NH). ^{13}C NMR (100.6 MHz, $CDCl_3$, ppm, room ternperature): 8.33 (q, CH_3); 8.53 (q, CH_3); 8.57 (q, CH_3); 9.02 (q, CH_3); 9.27 (q, CH_3); 9.37 (2q, 2CH_3); 22.24 (t, CH_2); 24.33 (t, CH_2); 26.24 (t, CH_2); 28.32 (t, CH_2); 28.45 (t, CH_2); 32.36 (t, CH_2); 33.38 (t, CH_2); 35.21 (t, CH_2); 35.41 (t, CH_2); 35.65 (t, CH_2); 36.30 (t, CH_2); 43.44 (s, CR_4); 44.66 (s, CR_4); 49.40 (s, CR_4); 49.67 (s, CR_4); 93.62 (s, N−*C*−CO); 102.69 (d, CH pyrrole); 103.21 (d, CH pyrrole); 103.58 (d, CH pyrrole); 104.64 (d, CH pyrrole); 106.33 (d, CH pyrrole); 107.53 (d, CH pyrrole); 128.52 (s, C pyrrole); 130.55 (s, C pyrrole); 133.31 (s, C pyrrole); 135.05 (s, C pyrrole); 136.34 (s, C pyrrole); 136.66 (s, C pyrrole); 183.55 (s, C=N); 216.65 (s, C=O).

Synthesis of 10. Compound **7** (1.13 g, 1.30 mmol), toluene (50 mL), and anilinium hydrochloride (0.35 g, 2.66 mmol) were combined at −60 °C, left to reach room temperature, and then heated at 50 °C for 3 days. LiCl was filtered out, the solvent evaporated to dryness, and the residue collected with *n*-hexane (20 mL). From the yellow solution yellow crystals formed, which were filtered and dried and structurally characterized by an X-ray analysis (0.27 g, 26%). Anal. Calcd for $C_{47}H_{64}N_6Zr$: C, 70.17; H, 8.04; N, 10.44. Found: C, 69.89; H, 8.13; N, 10.15. IR, ν(cm^{-1}): 1568 (PhNH); 1591 (PhNH); 1678 (C=N); 3169 (NH). ^{1}H NMR (200 MHz, C_6D_6, room temperature): δ 0.60−1.05 (m, 21 H, CH_3); 1.06 (s, 9 H, Bu^t); 1.15−2.60 (m, 22 H, CH_2); 6.05 (d, 1 H, ^3J = 3.1 Hz, CH); 6.17 (d, 1 H, ^3J = 3.1 Hz, CH); 6.33 (d, 2 H, ^3J = 3.0 Hz, CH); 6.39 (s, 1 H, CH); 6.64 (d, 2 H, ^3J = 7.7 Hz, *o*-H); 6.70 (d, 1 H, ^3J = 2.6 Hz, CH); 6.81 (t, 1 H, ^3J = 7.3 Hz, *p*-H); 7.11 (t, 2 H, ^3J = 7.7 Hz, *m*-H); 8.27 (s, 1 H, NH).

Synthesis of 11, Method A. $Mo(CO)_6$ (0.60 g, 2.27 mmol) was added to a THF (50 mL) solution of **2** (1.76 g, 2.23 mmol). The yellow color turned red after a few hours of stirring at room temperature. The solvent was evaporated, and the brown residue was collected with toluene (100 mL), heated at 80 °C for 30 min, and filtered while warm to eliminate a brick-red powder. The solvent was evaporated to dryness and the yellow powder extracted with *n*-hexane (50 mL), filtered, and dried (0.88 g, 52%). Crystals suitable for an X-ray analysis were grown from *n*-hexane/toluene. Anal. Calcd for $C_{44}H_{55}LiN_4OZr$: C, 70.00; H, 7.29; N, 7.42. Found: C, 69.11; H, 7.38; N, 7.41. IR, ν (cm^{-1}): 776 (Zr=O); 1589 (Py). ^{1}H NMR (200 MHz, THF-d_8, room temperature): δ 0.24 (t, 3 H, ^3J = 7.3 Hz, CH_3); 0.46 (t, 3 H, ^3J = 7.2 Hz, CH_3); 0.5−0.8 (m, 12 H, CH_3); 0.88 (t, 3 H, ^3J = 7.4 Hz, CH_3); 1.22 (m, 1 H, CH_2); 1.45 (m,1 H, CH_2); 1.55−2.2 (m, 11 H, CH_2); 2.23 (s, 3 H, CH_3 Tol); 2.41 (m, 1 H, CH_2); 2.54 (m, 1 H, α-CH_2); 2.76 (t, 2 H, ^3J = 7.2 Hz, β-CH_2); 3.1 (m, 1 H, α-CH_2); 5.69 (d, 1 H, ^3J = 3.0 Hz, CH); 5.79 (d, 2 H, ^3J = 2.9 Hz, CH); 5.83 (d, 1 H, ^3J = 3.1 Hz, CH); 6.09 (d, 1 H, ^3J = 2.8 Hz, CH); 6.33 (d, 1 H, ^3J = 2.7 Hz, CH); 7.07 (m, 5 H, CH Tol); 7.37 (d, 1 H, ^3J = 8.1 Hz; CH pyridine); 7.58 (d, 1 H, ^3J = 8.0 Hz; CH pyridine).

Synthesis of 11, Method B. A THF (150 mL) solution of **2** (4.15 g, 5.20 mmol) was stirred at −80 °C under a CO atmosphere for 1 h. The temperature was slowly allowed to reach 20 °C, and the solution was then stirred for 1 night. The solvent was evaporated and the residue collected with *n*-hexane (150 mL). The beige solid was extracted with refluxing *n*-hexane (100 mL) during 20 h. The elutant gave a white crystalline solid which was filtered and dried (1.10 g, 32%). The analytical data are identical to those reported in method A.

X-ray Crystallography for Complexes 2, 5 + 6, 7, 10, and 11. Suitable crystals of compounds **2**, **5** + **6**, **7**, **10**, and **11** were mounted in glass capillaries and sealed under nitrogen. The reduced cells were obtained with the use of TRACER.[20] Crystal data and details associated with data collection are given in Tables 1 and S1. Data were collected at room temperature (295 K) on a single-crystal diffractometer (Rigaku AFC6S for **2**, Siemens AED for **7**, and Enraf-Nonius CAD4 for **5** + **6**, **10**, and **11**). For intensities and background, individual reflection profiles[21] were analyzed. The structure amplitudes were obtained after the usual Lorentz and polarization corrections[22] and the absolute scale was established by the Wilson method.[23] The crystal quality was tested by scans showing that crystal absorption effects could not be neglected. The data were corrected for absorption using a semiempirical method[24] for complexes **2** and **11** and ABSORB[25] for **5** + **6**, **7**, and **10**. The function minimized during the least-squares refinement was $\sum w(\Delta F^2)^2$. Weights were applied according to the scheme $w = 1/[\sigma^2(F_o^2)+(aP)^2]$ $\{P = (F_o^2 + 2F_c^2)/3\}$ with a = 0.0796, 0.0691, 0.0661, 0.0773, and 0.1119 for complexes **2**, **5** + **6**, **7**, **10**, and **11**, respectively. Anomalous scattering corrections were included in all structure factor calculations.[26b]

(20) Lawton, S. L.; Jacobson, R. A. *TRACER (a cell reduction program)*; Ames Laboratory. Iowa State University of Science and Technology: Ames, IA, 1965.

(21) Lehmann, M .S.; Larsen, F. K. *Acta Crystallogr., Sect. A: Cryst. Phys., Diffr., Theor. Gen. Crystallogr.* **1974**, *A30*, 580.

(22) Data reduction was carried out on an IBM AT personal computer equipped with an INMOS T800 transputer.

(23) Wilson, A. J. C. *Nature* **1942**, *150*, 151.

(24) North, A. C. T.; Phillips, D. C.; Mathews, F. S. *Acta Crystallogr., Sect. A: Cryst. Phys., Diffr., Theor. Gen. Crystallogr.* **1968**, *A24*, 351.

(25) ABSORB, a Program for F_o Absorption Correction. Ugozzoli, F. *Comput. Chem.* **1987**, *11*, 109.

(26) (a) *International Tables for X-ray Crystallography*; Kynoch Press: Birmingham, England, 1974; Vol. IV, p 99; (b) p 149.

Scattering factors for neutral atoms were taken from ref 26a for non-hydrogen atoms and from ref 27 for hydrogens. Among the low-angle reflections no correction for secondary extinction was deemed necessary.

All calculations were carried out on an IBM-AT personal computer equipped with an INMOS T800 transputer and an ENCORE 91 computer. The structures were solved by the heavy-atom method starting from three-dimensional Patterson maps using the observed reflections. The refinement of the structures was carried out with SHELX92[28] and was based on the unique total data for **2**, **5** + **6**, and **7**. Refinements of **10** and **11** were based on the unique observed data.

Complex 2. Refinement was first done isotropically and then anisotropically for all non-H atoms except for the C23, C24 carbons of an ethyl group, which were found to be statistically distributed over two positions (A, B) isotropically refined with a site occupation factor of 0.5. Attempts to refine anisotropically these atoms led to fluctuating Δ/σ. One THF molecule (O1, C41, C42, C43, C44) was affected by disorder, which was solved by considering the carbon atoms statistically distributed over two positions (A, B) with a site occupation factor of 0.5. During the refinement the C−O and C−C bond distances of the disordered THF molecule were constrained to be 1.48(1) and 1.54(1) Å, respectively. All the hydrogen atoms but those related to the disordered carbon atoms, which were ignored, were located from difference Fourier maps and introduced in the final stage of refinement as fixed atom contributions (isotropic Us fixed at 0.10 Å^2). The final difference maps showed no unusual feature, with no significant peak above the general background.

Complexes 5 + 6. The number of molecules per unit cell ($Z = 4$) requires the molecule to have an imposed crystallographic symmetry. Excluding the centrosymmetry for chemical reasons, the structure was solved considering the zirconium atom to lie on a 2-fold axis of the centrosymmetric C2/*c* space group. The subsequent Fourier synthesis succeeded in revealing the alkali metal and the porphyrinogen moiety, indicating a severe disorder associated to the ethylic chains bonded to the C5 carbon. The disorder was interpreted as due to the simultaneous presence of both the α- and β-dimetalated structural isomers. The best fit was found by splitting the C11−C12 and C13−C14 ethyl groups over two positions (A, B) with site occupation factors of 0.75 and 0.25 corresponding to the presence of 75% and 25% of the α (A positions) and β (B positions) isomers. The site occupation factors were derived from the height of the peaks on a ΔF map calculated without the contribution of the C11 and C12 carbon atoms. Attempts to remove disorder adopting the noncentrosymmetric *Cc* space group and considering the two independent ethyl chains α- and β-bonded to zirconium were unsuccessful owing to the persistency of the centrosymmetry. So the model containing three α-metalated isomers and one β-metalated isomer *per* unit cell was considered the most satisfactory. The C25 and C28 carbons of a THF molecule (O2−C25···C28) were found to be statistically distributed over two positions (A, B) with site occupation factors of 0.6 and 0.4, respectively. Refinement was first done isotropically and then anisotropically for all non-H atoms. All the hydrogen atoms but those related to the disordered carbon atoms, which were ignored, were located from difference Fourier maps and introduced in the final stage of refinement as fixed atom contributions (isotropic Us fixed at 0.12 Å^2). The final difference maps showed no unusual feature, with no significant peak above the general background.

Complex 7. Refinement was first done isotropically and then anisotropically for all non-H atoms except for the disordered atoms. The two THF molecules were found to be affected by disorder. It was solved by splitting over two positions (A and B) the C44 and C45 carbons of a molecule and all the carbons of the other (C46−C49) (Figure 4). The "partial atoms" were isotropically refined with a site occupation factor of 0.5. During the refinement the C−O and C−C bond distances involving the disordered atoms were restrained to be 1.48(1) and 1.54(1) Å, respectively. All the hydrogen atoms except those related to the THF molecules, which were ignored, were located from difference Fourier maps and introduced in the final stage of refinement as fixed atom contributions (isotropic Us fixed at 0.10 Å^2). The final difference maps showed no unusual feature, with no significant peak above the general background.

Complex 10. Refinement was done first isotropically and then anisotropically for all non-H atoms. All the hydrogen atoms were located from difference Fourier maps and introduced in the final refinement as fixed atom contributions (isotropic Us fixed at 0.08 Å^2). The final difference map showed no unusual feature, with no significant peak above the general background.

Complex 11. Refinement was first done isotropically and then anisotropically for all non-H atoms except for the disordered atoms. The C12, C13, C28 carbon atoms of the macrocyclic ring and the C21, C22 carbon atoms of an ethylic chain were found to be statistically distributed over two positions (A, B) isotropically refined with a site occupation factor of 0.5. Isotropic refinement of the C1S−C7S toluene molecule of crystallization gave unaceptably high U values without any indication of disorder. This suggested a statistical distribution of toluene in the crystal lattice. The site occupation factor was therefore allowed to vary, resulting in a value of 0.6 corrresponding to an occupation of the 60% of unit cells. During the refinement the Ph ring was constrained to be a regular hexagon (C−C = 1.39(1) Å). All the hydrogen atoms except those related to the disordered carbon atoms and to the toluene molecule, which were ignored, were located from difference Fourier maps and introduced in the final stage of refinement as fixed atom contributions (isotropic U's fixed at 0.10 Å^2). The final difference maps showed no unusual feature, with no significant peak above the general background.

Final atomic coordinates are listed in Tables S2−S6 for non-H atoms and in Tables S7−S11 for hydrogens. Thermal parameters are given in Tables S12−S16, bond distances and angles in Tables S17-S21.[29]

Acknowledgment. We would like to thank the "Fonds National Suisse de la Recherche Scientifique" (Grant. No. 20-33420-92) for financial support.

Supplementary Material Available: Tables of experimental details associated with data collection and structure refinement (Table S1), fractional atomic coordinates (Tables S2−S11), thermal parameters (Tables S12−S16), and bond distances and angles (Tables S17−S21) (32 pages). This material is contained in many libraries on microfiche, immediately follows this article in the microfilm version of the journal, can be ordered from the ACS, and can be downloaded from the Internet; see any current masthead page for ordering information and Internet access instructions.

JA943536R

(27) Stewart, R. F.; Davidson, E. R.; Simpson, W. T. *J. Chem. Phys.* **1965**, *42*, 3175.

(28) Sheldrick, G. M. *SHELX-92: Program for Crystal Structure Refinement*; University of Göttingen, Germany, 1992.

(29) See paragraph at the end of the paper regarding supplementary material.